Water solubility, antioxidant activity and cytochrome C binding of four families of exohedral adducts of C_{60} and C_{70}†

Patrick Witte,[a] Florian Beuerle,[a] Uwe Hartnagel,[a] Russell Lebovitz,[b] Anastasia Savouchkina,[c] Sevda Sali,[c] Dirk Guldi,*[c] Nikos Chronakis[d] and Andreas Hirsch*[a,b]

Received 7th August 2007, Accepted 17th September 2007
First published as an Advance Article on the web 2nd October 2007
DOI: 10.1039/b711912g

Over the past decade, surface-modified, water soluble fullerenes have been shown by many different investigators to exhibit strong antioxidant activity against reactive oxygen species (ROS) *in vitro* and to protect cells and tissues from oxidative injury and cell death *in vivo*. Nevertheless, progress in developing fullerenes as *bona fide* drug candidates has been hampered by three development issues: 1) lack of methods for scalable synthesis; 2) inability to produce highly purified, single-species regioisomers compatible with pharmaceutical applications; and 3) inadequate understanding of structure–function relationships with respect to various surface modifications (*e.g.*, anionic *versus* cationic *versus* charge-neutral polarity). To address these challenges, we have designed and synthesized more than a dozen novel water soluble fullerenes that can be purified as single isomers and which we believe can be manufactured to scale at reasonable cost. These compounds differ in addition pattern, lipophilicity and number and type of charge and were examined for their water solubility, antioxidant activity against superoxide anions and binding of cytochrome C. Our results indicate that dendritic water soluble fullerene[60] monoadducts exhibit the highest degree of antioxidant activity against superoxide anions *in vitro* as compared with trismalonate-derived anionic fullerenes as well as cationic fullerenes of similar overall structure. Among the higher adducts, anionic derivatives have a higher antioxidant activity than comparable cationic compounds. To achieve sufficient water solubility without the aid of a surfactant or co-solvent at least three charges on the addends are required. Significantly, anionic in contrast to cationic fullerene adducts bind with high affinity to cytochrome C.

Introduction and background

Within a few years after the first production of fullerenes in macroscopic quantities[1] it was recognized that the extended conjugated π-system of C_{60} exhibits unusual potency for scavenging of radicals including reactive oxygen species (ROS).[2] The major impediment for the development of fullerene-based biological antioxidants has been the relative insolubility of C_{60} in either aqueous or lipid-based solvents. Early attempts to modify the surface of the fullerene by polyhydroxylation and hexasulfobutylation produced water-soluble fullerenes with good biological distribution and cell penetration.[3–10] These early classes of water soluble fullerenes exhibited surprisingly potent antioxidant and cytoprotective activities *in vivo*, including: 1) significant reduction of death and permanent tissue loss associated with severe ischemia/reperfusion injury resulting from complete blockage and subsequent re-opening of coronary[3] and carotid[4] vasculature; 2) protection of cultured neurons from glutamate excitotoxicity[5,6] and peroxide-induced injury to rat hippocampal slices;[7] 3) protection of small intestine from ischemia/reperfusion injury[8] and in intestinal grafts after transplantation;[9] and 4) protection of pulmonary tissue from pulmonary hypertension induced by chronic hypoxia[10] and bronchoconstriction due to exsanguination and acute blood loss.

One major drawback to development of pharmaceutical applications for polyhydroxylated and hexasulfobutyl fullerenes is that they have highly heterogeneous structures with respect to both the number of addends (polyhydroxyfullerenes) and the regioisomerism of the addends attached to the fullerene core (both classes). From a pharmaceutical perspective, the most significant advance in the development of fullerene-based antioxidants took place in the mid-1990s with the synthesis and characterization of methanofullerenes bearing terminal carboxy groups (carboxyfullerenes), a class of exohedral fullerene adducts that could be synthesized in a highly purified and chemically homogeneous form.[11–15] Furthermore, since the carboxyfullerenes can be generated as single regioisomers, it is possible to design and synthesize a wide variety of different three-dimensional structures and charge distributions to optimize structure–function

[a]*The Institut für Organische Chemie, Universität Erlangen-Nürnberg, Henkestrasse 42, D-91054, Erlangen, Germany. E-mail: andreas.hirsch@chemie.uni-erlangen.de*
[b]*C-Sixty Inc., Houston, USA*
[c]*Institut für Physikalische Chemie, Universität Erlangen-Nürnberg, Egerlandstrasse 3, D-91058, Erlangen, Germany*
[d]*Department of Chemistry, University of Cyprus, P. O. Box 20537, 1678, Nicosia, Cyprus*

† Electronic supplementary information (ESI) available: Synthesis procedures and characterization details of the precursor compounds **4**, **20–31**, **37–41**, **54** and **55** and the fullerene compounds **43–47**, **49–53** and **60–64**. See DOI: 10.1039/b711912g

relationships and minimize "off target" binding and toxicity. So far two carboxyfullerenes have been synthesized and investigated with respect to their antioxidant properties: 1) carboxyfullerenes C_3-[*e*,*e*,*e*-$C_{63}(COOH)_6$] (**1**) and D_3-[*trans*3,*trans*3,*trans*3-$C_{63}(COOH)_6$] (**2**).[13,15] Another prominent carboxyfullerene is the dendrofullerene **3**, which is very soluble in water and has been investigated with respect to a variety of biomedical properties.[14] In experiments similar to those described for fullerenols and hexasulfobutylated fullerenes, carboxyfullerenes **1** and **2** have been shown to exhibit the following therapeutic benefits linked to their antioxidant activities: 1) carboxyfullerenes locate preferentially to mitochondria[16] and can reconstitute mitochondrial superoxide dismutase protection from superoxide radicals in SOD2 genetically deficient mice;[17] 2) carboxyfullerenes are highly potent neuroprotective agents, preventing cell death across a variety of different neuronal types in disease models as diverse as Parkinson's, Alzheimer's, ALS, excitotoxicity, macular degeneration and stroke;[18–25] 3) carboxyfullerenes protect cells from damaging effects of UV and γ-irradiation;[26] 4) carboxyfullerenes protect from morbidity and mortality in the presence of overwhelming infection with both gram-positive and gram-negative organisms;[27–30] 5) carboxyfullerenes protect a variety of different cell types, including leukocytes, hepatocytes and renal tubular epithelial cells, from oxidative injury associated with chemical and biological agents.[31–33]

In the current manuscript, we describe our efforts to rationally design, test and optimize several novel types of carboxyfullerenes and cationic fullerenes for biological antioxidant and cytoprotective activities. In all cases, we have selected candidates and synthetic protocols that can be easily scaled and which can be used to manufacture a single highly purified fullerene species.

Results

Design and synthesis of water soluble C_{60} trisadducts involving an *e*,*e*,*e*-addition pattern

The fullerene trisadduct *e*,*e*,*e*-trismalonic acid (**1**) (so-called C3) has been shown to be an effective neuroprotectant both in cultured CNS cells and in whole animal models.[16–35] This molecule can be synthesized very easily in large quantities by first allowing a macrocyclic trismalonate to react regioselectively with three adjacent equatorial [6,6] double bonds of the fullerene core and subsequent hydrolysis of the ester groups.[11,15] However, the potential use of C3 as a drug candidate is accompanied by two severe drawbacks: 1) hands-on experience with this compound has shown that the malonic carboxylic groups are rather unstable and easily decarboxylate to $C_{63}H(COOH)_5$, $C_{63}H_2(COOH)_4$ and $C_{63}H_3(COOH)_3$ as mixtures of several stereoisomers. Some of them show significant cytotoxicity;[36] 2) **1** is very polar, exhibiting on average more than five negative charges at neutral pH, and in the absence of further lipophilic components, presents disadvantages with respect to bioavailability. To overcome these problems we recently set out with a new concept for the synthesis of stable water soluble *e*,*e*,*e*-adducts with a tunable balance of hydrophilicity and lipophilicity.[37] The idea was to use tripodal trismalonate tethers where the reactive malonate groups are connected *via* alkyl spacers to a benzene core. The second ester moiety of each malonate is terminated by another functional, *e.g.*, protecting group. The corresponding *e*,*e*,*e*-trisadducts derived from the very regioselective threefold Bingel cyclopropanation possess two distinct addend zones, namely, the polar zone characterized by the focal benzene moiety and the equatorial zone, which can be used for the introduction of *e.g.* carboxylic or pyridinium groups

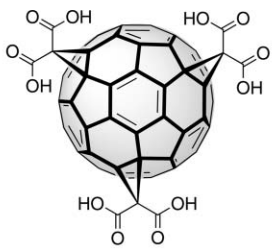

1

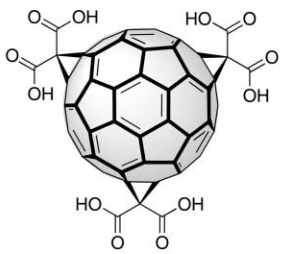

2

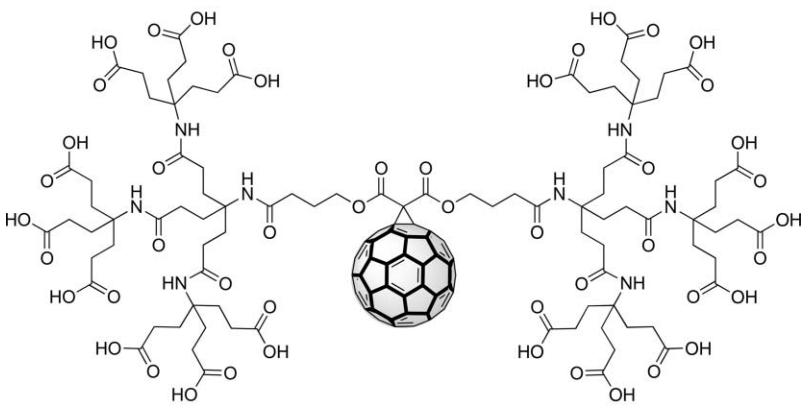

3

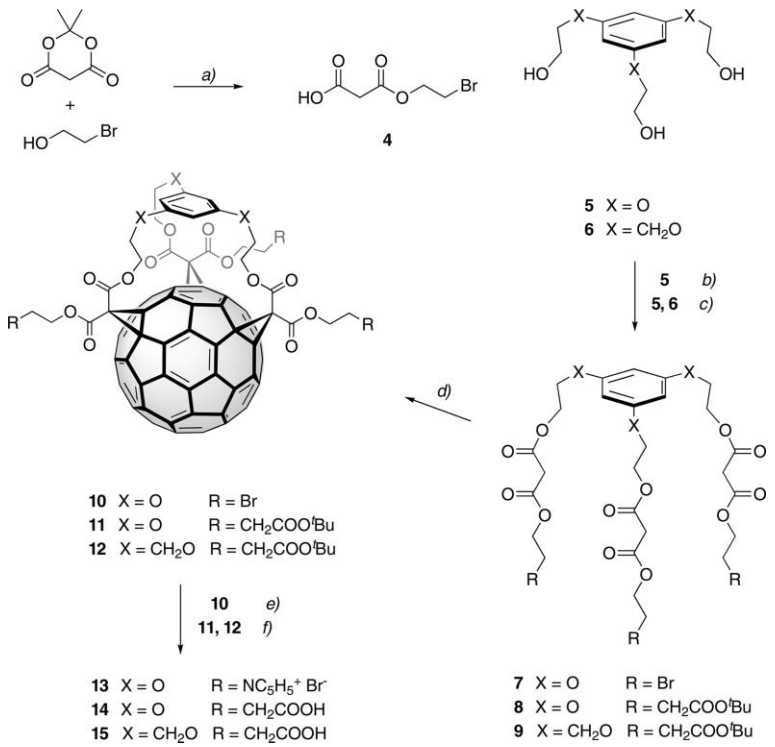

Scheme 1 Synthesis of water soluble trisadducts involving an *e*,*e*,*e* addition pattern: *a*) toluene, reflux; *b*) **4**, DCC, DMAP, THF, 0 °C → rt; *c*) ^{t}BuOOC(CH$_2$)$_3$OOCCH$_2$COOH, DCC, DMAP, THF, 0 °C → rt; *d*) C_{60}, I_2, DBU, toluene; *e*) pyridine, 60 °C, four days; *f*) HCOOH, two days.

which guarantee water solubility of the entire architecture. The whole sequence of this functionalization process is represented in Scheme 1. Using this approach, we have already synthesized the two *e*,*e*,*e*-triscarboxylates **14** and **15**, differing in the connection of the malonate side arms to the focal benzene core.[37] Both adducts **14** and **15** are very soluble in water at pH 8 due to the complete deprotonation. Compared to **1** they are very stable; furthermore, they exhibit an additional lipophilic region in the polar addend zone. For comparison we have now developed the new adduct **13** which has a related building principle similar to **14** and **15**, but contains cationic pyridinium groups in the equatorial addend zone for the establishment of water solubility. For this purpose, malonate **4** bearing a bromo terminus was synthesized by the reaction of Meldrum's acid with bromoethanol. Subsequent ester coupling with the triol **5** afforded the tripodal trismalonate tether **7**. Cyclopropanation of C_{60} with **7** leads to the regioselective formation of precursor adduct **10** as the only isomer. The final transformation into the trispyridinium salt **13** was accomplished in 95% yield. This triscationic fullerene derivative is very soluble in water. The formation of the stable red colored solutions can be promoted even further by using neutral and non-buffered water. Structural characterization of **4**, **7**, **10** and **13** was carried out by ^{1}H NMR, ^{13}C NMR and UV/Vis spectroscopy as well as by mass spectrometry.

Design and synthesis of water soluble C_{60} monoadducts carrying amphiphilic malonate addends

Although the synthesis of the dendrofullerene **3** was published several years ago,[14] few, if any investigations on its antioxidant properties have been published to date. Compared to **1** and **2**, dendrofullerene **3** exhibits a much higher water solubility, is very stable and has only one instead of three addends, making it in principle a much more potent radical scavenger. As a consequence, we would expect **3** to be a more potent antioxidant compared with **1** and **2**. However, at neutral pH it bears on average 16 negative charges, and this high degree of polarity could cause significant pharmacokinetic drawbacks including limited biodistribution within lipid rich regions. In seeking to enhance the pharmacokinetic properties of **3**, we decided to synthesize a series of variants such as the first generation analogue **16** as well as several amphiphilic adducts containing both polar dendritic and lipophilic moieties to enhance cell and tissue accessibility. Like **3**, adduct **16** can be easily prepared by Bingel cyclopropanation of C_{60} with the corresponding *tert*-butyl protected first generation malonate and the subsequent acidic cleavage of the *tert*-butyl groups.

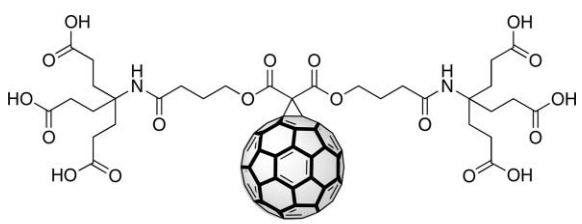

16

The general strategy for the synthesis of the amphiphilic water soluble monoadducts is shown in Scheme 2. The crucial point is the facile generation of unsymmetrical malonate precursors that serve as addends. Previously, we have prepared unsymmetrical malonates by the successive esterification of malonic acid with

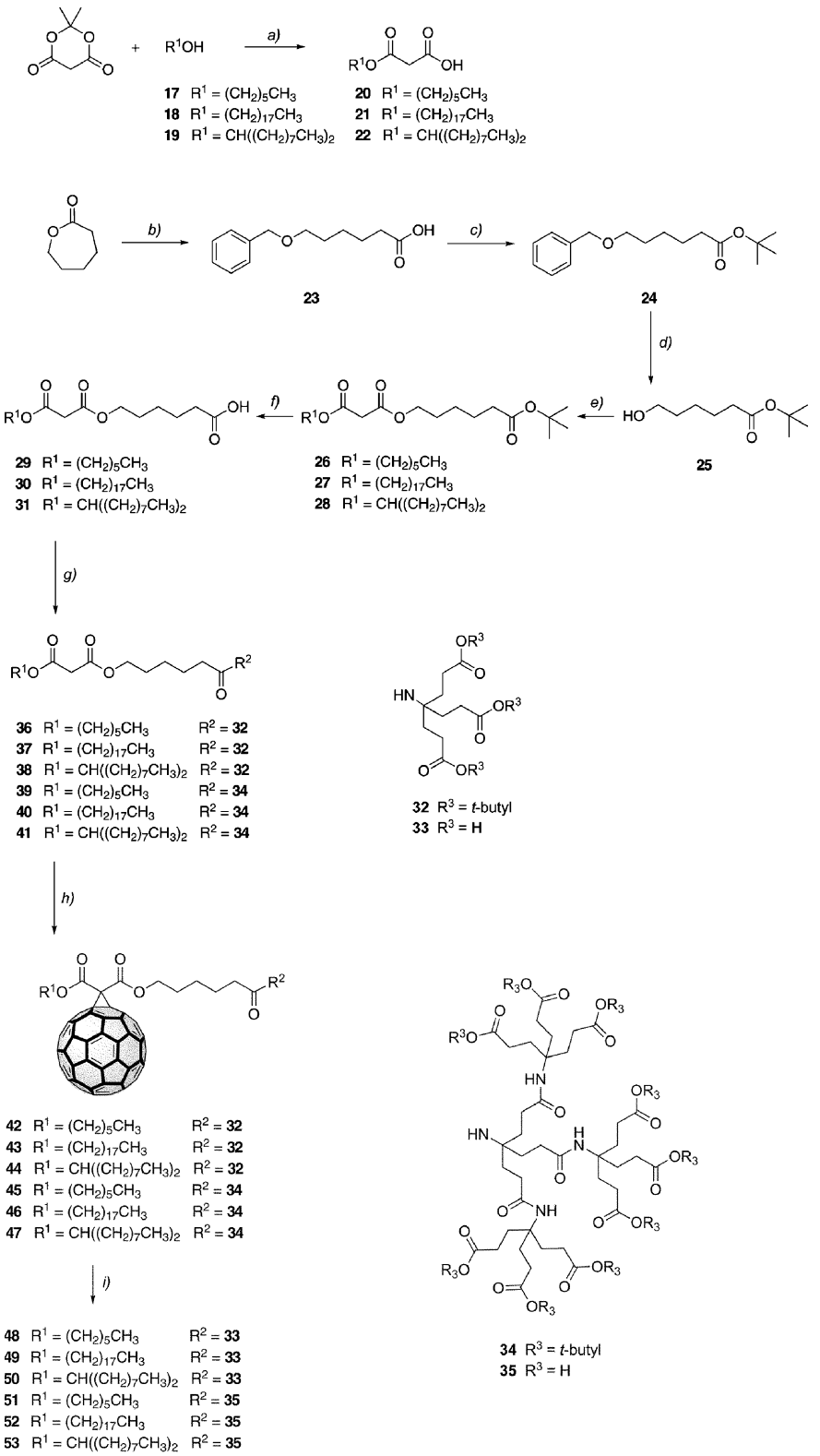

Scheme 2 Synthesis of water soluble monoadducts carrying amphiphilic malonate addends: a) 115 °C, 3 h; b) benzyl bromide, KOH, toluene, reflux, 48 h; c) isobutene, H_2SO_4, CH_2Cl_2, rt, 24 h; d) H_2, 10% Pd/C, methanol, rt, 48 h; e) DCC, DMAP, CH_2Cl_2, 0 °C → rt, 24 h; f) CF_3COOH, CH_2Cl_2, rt, 12 h; g) **32**/**34**, EDC, DMAP, 1-HOBt, CH_2Cl_2–THF 1 : 1, 0 °C → rt, 48 h; h) C_{60}, CBr_4, DBU, toluene, rt, 8 h; i) formic acid, rt, 48 h.

different alcohols.[38] However, this approach led in a number of cases to separation problems and unsatisfactory yields. In this new approach we started with Meldrum's acid which was allowed to react with a long chain alcohol to give the monoalkyl malonates **20–22** in 93–98% yields. As the second terminus, an alcohol was required that contains a protected carboxylic group in its

periphery serving as anchor point for the introduction of the dendritic building blocks. This was accomplished by treating ε-caprolactone with benzyl bromide leading to the formation of **23**. The protection of the terminal carboxylic groups was carried out by reaction with isobutene to give the *tert*-butyl ester **24**. After removal of the benzyl group by catalytic hydrogenation with Pd/C as catalyst, the deprotected alcohol **25** was obtained in 71% overall yield. DCC/DMAP coupling of **25** with the monomalonates **20–22** led to the formation of the unsymmetrical bismalonates **26–28**, which after acidic cleavage of the *tert*-butyl groups were allowed to react with the dendritic amines[39] **32** and **34** to give the unsymmetrical bismalonates **36–41**. Further Bingel cyclopropanation furnishes the monoadducts **42–47**. The final step in the synthesis of the amphiphilic fullerenes **48–53** was the acidic (trifluoroacetic acid) deprotection of the peripheral carboxylic groups of **42–47**. Unambiguous structural characterization of the target compounds was achieved by ^{1}H NMR, ^{13}C NMR and UV/Vis spectroscopy as well as by mass spectrometry. While compounds **51–53** bearing the second generation dendron show very good solubility in water at pH = 7.2, the first generation analogs **48–50** with three peripheral carboxylic groups only are not soluble in water. However, to promote water solubility of these compounds, it is possible to first dissolve them in a small amount of DMSO followed by the addition of water. Such solutions are stable for weeks.

Synthesis of mono- and bisadducts of C_{60} and C_{70} bontaining polyether malonates as addends

We became very interested in the question of whether fullerene derivatives with neutral addends would behave differently with respect to the antioxidant properties when compared to the ionic compounds described thus far. If their performance as antioxidant were similar to that of ionic compounds, they could have a number of advantages, especially improved bio-availability and pharmacokinetics. For example, neutral compounds should be superior with respect to the penetration of cell membranes as well as vascular barriers such as the gut or the blood–brain barrier. Although the water solubility of neutral adducts was expected to be considerably lower than that of charged derivatives, the potential pharmaceutical applicability of these compounds is not necessarily reduced, since many known drug molecules are insoluble in water. A suitable formulation of these molecules such as application in the presence of surfactants or proteins is easily conceivable. In addition to the investigation of neutral adducts, we also decided to look also whether changes within the fullerene core such as addition pattern or nature of the fullerene has an influence on the antioxidant properties. For this purpose we employed also C_{70} as the basic fullerene as well as different regioisomeric bisaddition patterns of the C_{60} and C_{70} clusters (Fig. 1).[2]

For these purposes, we chose to utilize triethylene glycol units terminated with a hydroxy group as neutral side chain in the malonate. The corresponding precursor malonate **55** was synthesized by the initial monoprotection of triethyleneglycol with *tert*-butyldimethylsilyl chloride (TBDMSCl) (Scheme 3). The resulting alcohol **54** was then converted to **55** by the reaction with malonyl dichloride. Coupling of **55** with a slight excess of C_{60} led to the formation of the monoadduct **56** in 40% yield, which was subsequently subjected to deprotection in a solution

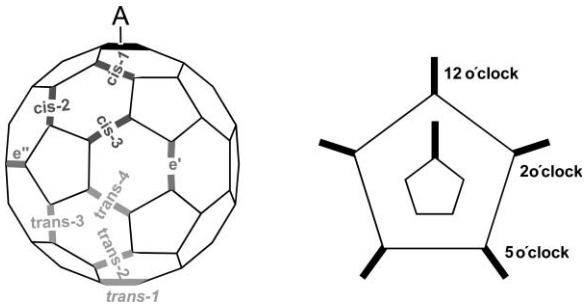

Fig. 1 Representation of regioisomeric bisaddition patterns of C_{60} and C_{70}.

of hydrochloric acid in tetrahydrofuran to give the desired derivative **57**. Use of a 2.2-fold excess of **55** on the other hand afforded a regioisomeric mixture of bisadducts **58** as main reaction products. From this mixture, the regioisomers **58a–d** with the addends bound in *trans*-2-, *trans*-3-, *trans*-4- and *e*-positions[40] were isolated by preparative HPLC. The target compounds **59a–d** where subsequently prepared by treatment of the corresponding precursor adduct **58** with a mixture of trifluoroacetic acid and hydrochloric acid. Structural characterization of the monoadducts **56** and **57** as well as of the bisadducts **58** and **59** was achieved by ^{1}H NMR, ^{13}C NMR and UV/Vis spectroscopy as well as by mass spectrometry. The deprotected mono- and bisadducts are insoluble in water and only slightly soluble in methanol and ethanol. However, water solubility can be promoted or enhanced by the addition of TWEEN20 as a surfactant. We prepared the corresponding methyl ether **60** for comparison as a representative of this group with even less polar side chains.

Treatment of C_{70} with 0.8 equivalents of **55** produced the monoadduct **61** as the major regioisomer; the malonate in this case is bound to most reactive [6,6]-sites with the highest degree of pyramidalization at the pole in 37% yield (Scheme 4). After purification by flash chromatography and acidic deprotection, the corresponding diol **62** was obtained in 75% yield. If a slight excess of **55** was used for the cyclopropanation of the fullerene, a mixture of regioisomeric bisadducts **63** was formed as the major reaction products. Among these the 2 o'clock, 5 o'clock and 12 o'clock isomers[41] **63a–c** were isolated by HPLC as the major isomers. Preferred formation of C_{70} bisadducts in the form of 2 o'clock, 5 o'clock and 12 o'clock isomers with the addends bound at the most reactive sites of the opposite poles has previously been reported by Diederich and co-workers using other types of malonate addends.[41] The final acidic deprotection of the TBDMS-groups produced the tetraols **64a–c**. Structural characterization of the monoadducts **61** and **62** as well as of the bisadducts **63** and **64** was achieved by ^{1}H NMR, ^{13}C NMR and UV/Vis spectroscopy as well as by mass spectrometry. The solubility behavior of the deprotected C_{70} adducts **62** and **64** is comparable to those of the corresponding C_{60} analogs.

Synthesis of water-soluble oxo-tetrapiperidinyl-[60]fullerenes

We discovered some time ago that C_{60} reacts with an excess of amines in the presence of O_2 to form oxo-tetraamino-[60]fullerenes of the general structure shown in Fig. 2.[42] This addition pattern is completely different from those modified fullerenes presented

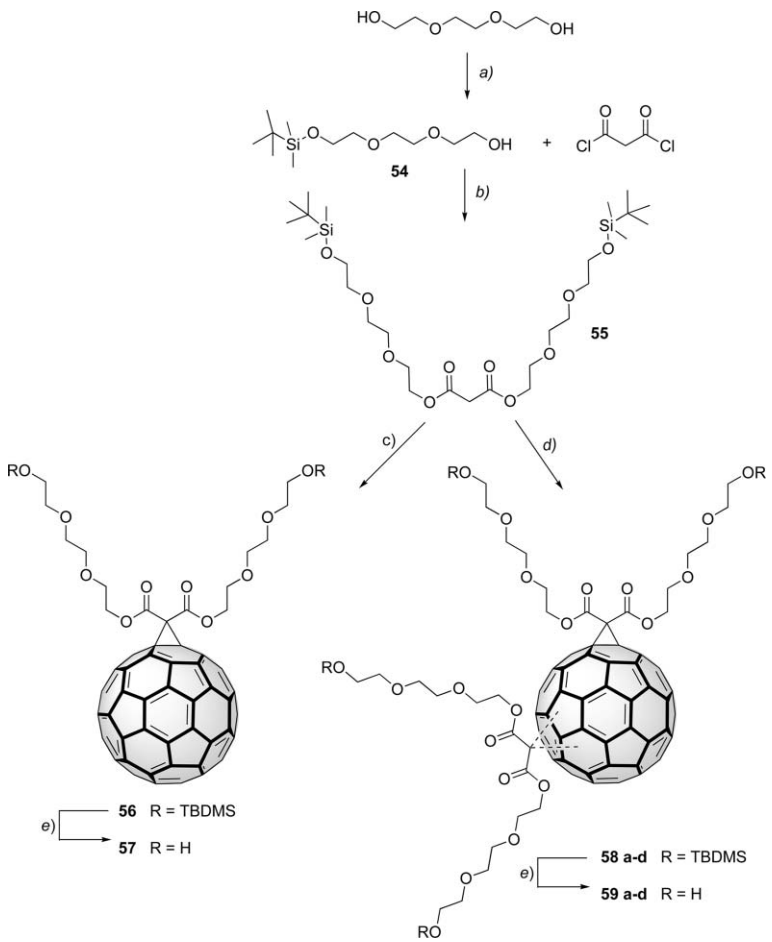

Scheme 3 Synthesis of mono- and bisadducts of C_{60} containing polyether malonates as addends: *a*) imidazole, TBDMSCl, 0 °C → rt, DMF; *b*) NEt_3, 0 °C → rt, CH_2Cl_2; *c*) 0.8 eq **55**, C_{60}, CBr_4, DBU, toluene; *d*) 2.2 eq **55**, C_{60}, CBr_4, DBU, toluene; *e*) 2 M HCl, THF; **a** = *trans*-2-, **b** = *trans*-3-, **c** = *trans*-4-, **d** = *e*-isomer.

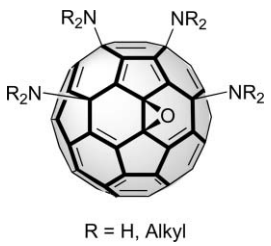

Fig. 2 General structure of an oxo-tetraamino-[60]fullerene obtained as major product by the treatment of C_{60} with amines in the presence of O_2.

thus far, and offers an opportunity to study antioxidant properties of another novel class of modified fullerenes. As a consequence it seemed worthwhile to synthesize a water soluble variant of this adduct type.

In order to do so we followed an optimized procedure for the synthesis of oxo-tetraamino-[60]fullerenes published recently by Isobe *et al.*[43] For the introduction of water solubility we used the protected amino piperidine **65** (Scheme 5). Treatment of C_{60} with 4 eq. of **65** in a mixture of DMSO and chlorobenzene in the presence of O_2 produced the adduct **66** in 80% yield. Subsequent deprotection of the BOC groups led to the formation of the ammonium salt **67**, which is very soluble in methanol and ethanol and slightly soluble in acidic water (pH 4). In order to achieve pH-independent water solubility, **67** was treated with MeI in the presence of $KHCO_3$ to give **68**, which is very soluble in water over a wide pH range. Characterization of the oxo-tetrapiperidinyl-[60]fullerenes **66–68** was carried out by ^1H NMR, ^{13}C NMR and UV/Vis spectroscopy as well as by mass spectrometry.

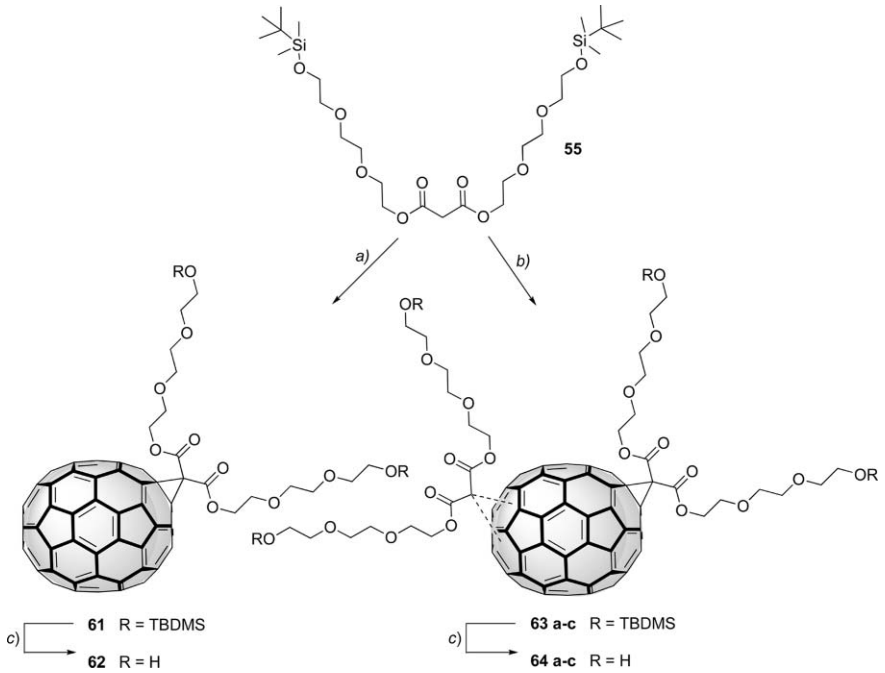

Scheme 4 Synthesis of mono- and bisadducts of C_{70} containing polyether malonates as addends: *a*) 0.8 eq **55**, C_{70}, CBr_4, DBU, toluene; *b*) 2.7 eq **55**, C_{70}, CBr_4, DBU, toluene; **a** = 2 o'clock-, **b** = 5 o'clock-, **c** = 12 o'clock isomer.

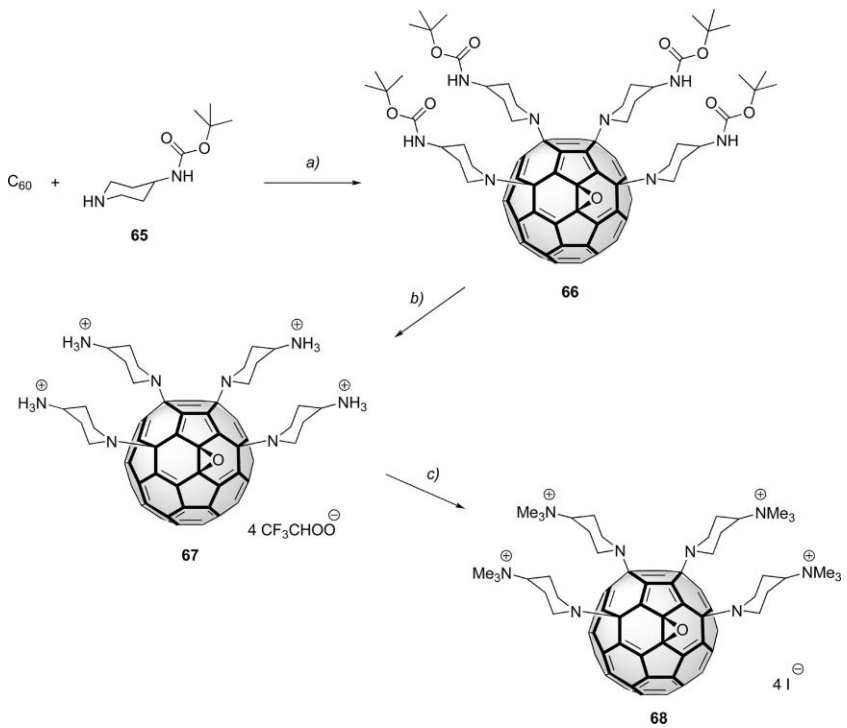

Scheme 5 Synthesis of oxo-tetrapiperidinyl-[60]fullerenes: *a*) C_{60}, 4 eq **65**, DMSO–PhCl 1 : 4, O_2 (20 min), rt 12 h; *b*) TFA, CH_2Cl_2; rt; *c*) $KHCO_3$, MeI, MeOH, 40 °C.

Antioxidant properties of water-soluble fullerenes

The superoxide anion is generally considered to be the predominant ROS species produced within cells, and at least one water soluble fullerene, namely the trisadduct C3 (**1**), has been shown to offer protection from oxidative injury in superoxide dismutase (SOD2) knockout mice exposed to high levels of this radical species.[17] To evaluate the relative antioxidant capabilities of our new water soluble derivatives and to understand critical structure–function relationships related to antioxidant activity

in a biological context, we focused initially on the ability of various fullerenes to remove or reduce the free-radical activities of superoxide in biological buffers. The standard assay to investigate the superoxide quenching ability of an antioxidant is based on xanthine/xanthine oxidase to generate superoxide causing the reduction of cytochrome C.[44] This process is followed photometrically by looking at the changes in intensity of the absorption band of reduced cytochrome C at 550 nm. Using this protocol we compared our new fullerenes and dendrofullerene **3** with trisadduct **1** as standard. The results are summarized in Table 1 and allow conclusions to be drawn concerning a structure–function relationship. Increasing the number of addends on the fullerene which leads to an increased rupture of the conjugated π-system causes a decreasing ability of superoxide quenching. For example, in the case of carboxyfullerenes, dendritic monoadducts such as **3**, **16**, **51–53** are more effective than *e*,*e*,*e*-trisadducts like **1**, **14** and **15** (Table 1, Fig. 3). In the case of the mono- and bisadducts of C_{60} and C_{70} carrying oligoethylene glycol addends, we observe that the monoadducts **57** ($IC_{50} = 64\ \mu M$) and **62** ($IC_{50} = 32\ \mu M$) are more effective than the corresponding bisadducts **59** and **64**. Significantly, the antioxidant activity within a series of bisadducts drops with increasing distance of the addends on the fullerene core. For example, the very remote *trans*-2 binding realized in the C_{60} bisadduct **59a** causes low activity ($IC_{50} = 789\ \mu M$), whereas equatorial binding leads to a considerable increase in activity ($IC_{50} = 62\ \mu M$). The cationic fullerenes investigated here are generally less effective antioxidants in this assay compared with anionic fullerenes of similar structure. For example, the oxo-tetrapiperidinyl adduct **67** is a less effective antioxidant at pH = 6 ($IC_{50} = 47\ \mu M$) than at pH = 7.4 ($IC_{50} = 35\ \mu M$), where the fourfold protonation is incomplete. Similarly, the corresponding permethylated derivative **68** whose tetracationic state is pH independent, exhibits antioxidant activity comparable to **67** at the lower pH ($IC_{50} = 45\ \mu M$). Moreover, the triscationic

Table 1 IC_{50} values for the superoxide quenching activities of fullerene derivatives in xanthine/xanthine oxidase assays

Compound	IC_{50}/μmol
1	18.5
2	16.8
3	11.0
13	202.0
14	36.5
15	56.0
16	6.2
49	24.0
50	26.1
51	13.3
52	15.4
53	14.7
57	64.0
60	289.0
62	32.0
67 (pH 7.4)	35.0
67 (pH 6.0)	47.0
68	45.4
59a	789.0
59b	139.6
59c	55.5
59d	62.5
64a	50.0
64c	76.9

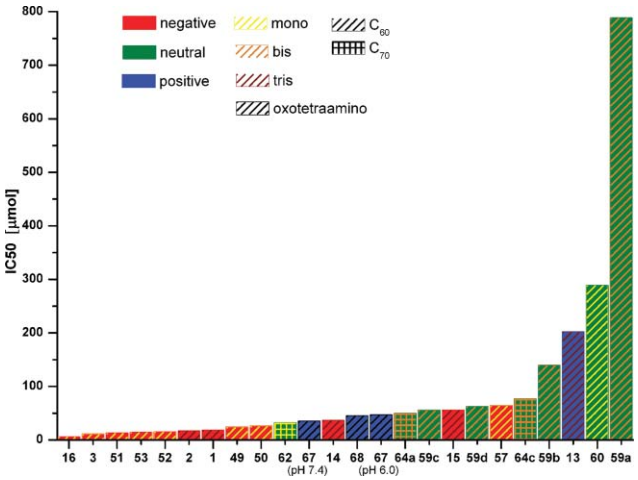

Fig. 3 IC_{50} values for the superoxide quenching activities of fullerene derivatives in xanthine/xanthine oxidase assays.

e,*e*,*e*-trisadduct **13** ($IC_{50} = 202\ \mu M$) is significantly less effective as an antioxidant compared with its anionic counterparts **14** ($IC_{50} = 36.5\ \mu M$) and **15** ($IC_{50} = 56\ \mu M$) as well as the trisadduct standard **1** ($IC_{50} = 18.5\ \mu M$).

Cytochrome C binding

The relatively low IC50 activity observed for cationic water soluble fullerenes in the cytochrome C-based superoxide quenching assay compared with anionic fullerenes of almost identical regioisomeric structure was somewhat surprising given the expectation that positively charged compounds would be more likely to capture negatively charged superoxide anions. These expectations had been shown previously for addition of hydroxyl radicals to the fullerene core, where positively charged fullerenes exhibited greater rate constants for the radical addition reaction.[45] In this regard it is important to ask whether the activity of the fullerene adducts against the xanthine/xanthine oxidase/cytochrome C assay is exclusively due to the ability of quenching superoxide or due to additional effects caused by the interplay of the components present in the matrix. One possible interaction, which may play a crucial role both in such an assay and also in biological systems is electrostatic interaction between the charged fullerene derivatives and the positively charged cytochrome C. In a previous investigation we have studied the electrostatic binding and photoinduced electron transfer between cytochrome C and **3** and related anionic fullerene adducts.[38] Indeed strong electrostatic binding with an association constant of $K_s = 1.7 \times 10^5\ M^{-1}$ (pH = 6) was observed.

We therefore wanted to complement the aforementioned results of the assay by subjecting the different fullerene derivatives to binding studies with cytochrome C. In the case of intact cytochrome C, the protein shell that surrounds the iron(II)/iron(III)-porphyrin hampers the direct electronic interactions that are readily observed, between fullerenes and unbound porphyrins. Therefore, we turned to excited interactions, which, however, necessitated the implementation of a zinc(II)-porphyrin chromophore rather than the iron(II)/iron(III)-porphyrin. This was deemed necessary, because iron(II) or iron(III) centers tend to deactivate excited states efficiently.

In the corresponding experiments, aqueous solutions of Zn(II)-cytochrome C (*i.e.*, 0.9–1.4 × 10^{-6} M) buffered at pH 7.2 were titrated with variable concentrations of the different fullerene derivatives (*i.e.*, 0.7–22.4 × 10^{-6} M). Regardless of the strength of fullerene/Zn(II)-cytochrome C interactions using other assays, the absorption spectra were not sufficiently sensitive to detect these interactions, and are best described as the linear superimposition of the component spectra, namely, fullerene and Zn(II)-cytochrome C. In particular, Zn(II)-cytochrome C absorptions are seen at 424, 545 and 580 nm. Those of the fullerenes depend strongly on the number of functional addends (*i.e.*, mono- *versus* tris-addition) and the respective addition pattern—see Experimental section for details.

Fluorescence-quenching experiments provided a more sensitive and consistent assay for fullerene/Zn(II)-cytochrome C interactions. For Zn(II)-cytochrome C, recording the typical fluorescence pattern of a zinc(II)-porphyrin with maxima at 585 and 644 nm and with high quantum yields of *ca.* 0.04, demonstrates the ability of this method to measure Zn(II)-porphyrin photoactivity inside of the protein matrix. In the presence of the fullerene derivatives, a non-linear quenching of the Zn(II)-cytochrome C centered fluorescence is clearly discernable (Fig. 4). It is important to note that the fluorescence emission spectrum remains constant throughout the titrations, although the amplitude varies due to quenching by the fullerenes. This nicely mirrors the trend seen in the absorption spectra, where no notable impact due to fullerene binding was seen on the absorption spectra. It is important in this context to consider the mechanism of fluorescence quenching of Zn(II)-cytochrome C in the presence of fullerenes: past work has provided thermodynamic, kinetic and spectroscopic evidence in support of an intra-ensemble charge separation that evolves between the photoexcited Zn(II)-cytochrome C and the electron accepting fullerene **3**.[38]

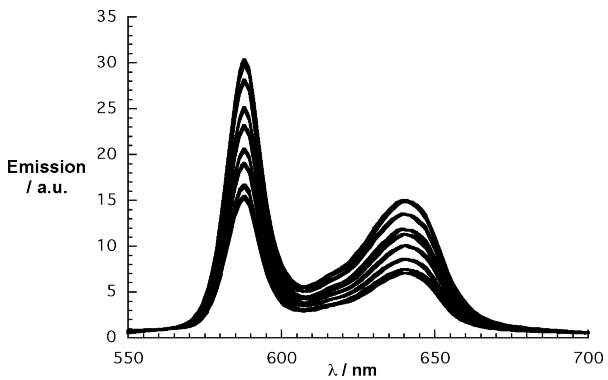

Fig. 4 Room temperature fluorescence spectra of 1.4 × 10^{-6} M Zn(II)-cyt C in aqueous solutions in the presence of variable concentrations of **49** (*i.e.*, 0, 3.9 × 10^{-6}, 5.4 × 10^{-6}, 6.9 × 10^{-6}, 8.5 × 10^{-6}, 9.2 × 10^{-6}, 1.2 × 10^{-5}, 1.3 × 10^{-5} M); excitation wavelength 420 nm.

In the next step, the non-linear quenching dependences were used to determine the binding constants (*i.e.*, K_a) for forming Zn(II)-cytochrome C/fullerene donor–acceptor ensembles held together by electrostatic forces (Table 2)—see Fig. 5. At first glance, the positively charged fullerene derivative **13** gives rise to binding constants below our detection limit of *ca.* 10^2 M^{-1}. This is rationalized on the basis of repulsive interactions between equally charged donor and acceptor constituents. On the other hand, all

Table 2 Binding constants and fluorescence lifetimes of Zn(II)-cyt C/fullerene complexes

Compound	K_a[a]/M^{-1}	Fluorescence lifetimes/ns	K_a[b]/M^{-1}	Net charge
16	2.2 × 10^7	0.45	4.3 × 10^7	6−
52	1.8 × 10^6	0.97	1.2 × 10^6	9−
1	1.5 × 10^6	0.25	8.6 × 10^5	6−
15	1.5 × 10^6	0.39		3−
14	1.3 × 10^5			3−
49	8.2 × 10^4	0.76		3−
13	<10^2			3+

[a] Steady-state fluorescence measurements. [b] Time-resolved fluorescence measurements

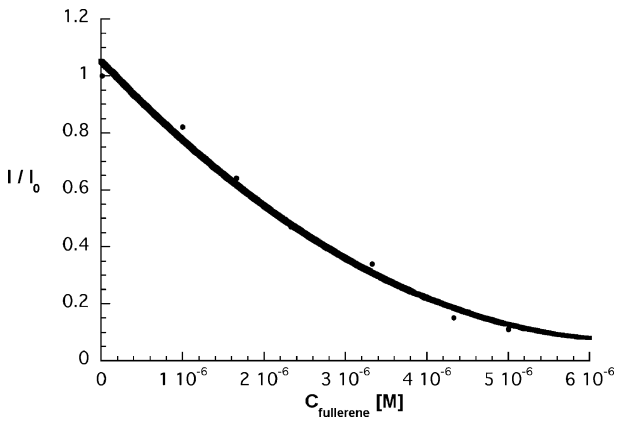

Fig. 5 A plot of the change in fluorescence intensity as a ratio of I/I_0 *versus* **52** concentration, the solid line represents the estimated curve fit obtained by non-linear least-squares analysis.

negatively charged fullerene derivatives (*i.e.*, **1**, **14**, **15**, **16**, **49**, **52**) reveal binding constants that ranged from 8.2 × 10^4 M^{-1} all the way to 2.2 × 10^7 M^{-1}.

A closer look allows for some conclusions based on structure–function relationships. All fullerene derivatives that bear three negative charges (*i.e.*, **14**, **15** and **49**) exhibit the lowest binding constants. It is interesting to note that the more flexible arrangement of the three carboxylic groups in **14** and **15** rather than the topologically more predefined motif in **49** (8.2 × 10^4 M^{-1}) results in a more synergistic binding pattern.

Placing, however, more than three negative charges on the fullerene further augments the binding: when comparing, for instance, **49** with **52** (1.8 × 10^6 M^{-1}) a more than 20-fold enhancement is seen. This argument is in line with the presence of eight positive charges that are located within the docking station of cytochrome C in general. In strong contrast to this conclusion, however, are the high binding constants of 1.5 × 10^6 M^{-1} and 2.2 × 10^7 M^{-1} for **1** and **16**, respectively. Both fullerene derivatives carry only six carboxylic groups, that is, three less than are present in **52**. Also notable is the topology of the addends in **1** and **16**: the six carboxylates in **1** are more evenly spread over the fullerene core although in a still rather rigid pattern. In **16**, which undoubtedly gives rise to the strongest binding, the two dendritic wedges may adjust flexibly to the binding sites of the cytochrome C pocket.

Independent confirmation was gathered using time-resolved fluorescence experiments (Table 2, Fig. 4). In particular, the Zn(II)-cytochrome C fluorescence lifetime was measured in the absence and presence of the electron accepting fullerene derivatives. When no fullerene was present we recorded fluorescence time profiles that are well fitted by a mono-exponential decay function. A lifetime of 2.2 ± 0.2 ns was determined under such conditions. In contrast, adding any of the studied fullerene derivatives led to fluorescence decays that were only reasonably fitted—with a χ^2 value of close to 1—by a bi-exponential function. Here, a long-lived component (*i.e.*, 2.2 ± 0.2 ns) and a short-lived component were registered. Interestingly, the exact value of the short-lived component was found to be dependent on the structure of the fullerene derivative. The largely different reduction potentials of mono- (*i.e.*, **16**, **49** and **52**) *versus* trisadducts (*i.e.*, **15** and **1**) should be considered, since they exert a major impact on the driving force for the electron transfer deactivation of the Zn(II)-cytochrome C singlet excited state. Moreover, a closer donor–acceptor separation also effects the electron transfer deactivation—please compare **1** (0.25 ns) with **15** (0.39 ns) or **16** (0.45 ns) with **49** (0.76 ns) (Table 2).

Throughout the titration experiments the two lifetimes remained constant. The only variable is the relative ratio between the long-lived and short-lived components. The long-lived component decreased continuously, while the short-lived component increased simultaneously. Similar to the steady-state experiments, the differing ratios were used to derive the binding constants (Fig. 6). Notably, an excellent agreement with the steady-state analysis is observed for the tested systems **52** (1.2×10^6 M^{-1}), **16** (4.3×10^7 M^{-1}) and **1** (8.6×10^5 M^{-1}). This confirmation carries even more weight when considering the vastly different fluorescence lifetime (*i.e.*, electron transfer rates) of 0.97 ns (**52**), 0.45 ns (**16**) and 0.25 ns (**1**).

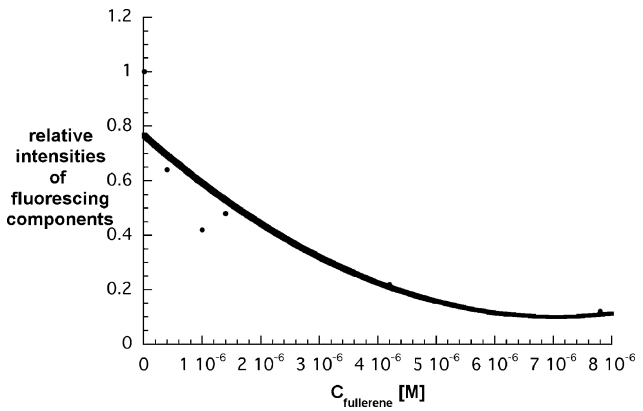

Fig. 6 A plot of the change in relative fluorescence intensities *versus* **52** concentration, the solid line represents the estimated curve fit obtained by non-linear least-squares analysis.

Discussion

The preponderance of data from biological systems strongly indicates that water soluble fullerenes can protect cells and tissues from injury and death related to chemical and biological insults including ischemia–reperfusion, direct oxidative injury, radiation injury (UV and γ) and chemical toxins such as adriamycin.[3–10,14,16–35] It has been assumed that the mechanism underlying this broad cytoprotection is directly related to the scavenging of reactive oxygen species by water soluble fullerenes, although the evidence underlying this assumption has been more circumstantial than direct. Our current work was initially intended to address the structure–function relationships underlying antioxidant activity for a subset of water soluble fullerenes against superoxide, but our observations have led us to understand also that direct interactions of the fullerene derivatives with charged redox proteins like cytochrome C may play an important role as well. We have described the design and synthesis for a number of novel water soluble fullerenes with the ultimate goal of assessing their potential as therapeutic antioxidants and cytoprotective drugs. Multiple independent factors are likely to play a role for each fullerene species, and these include: redox potential, size, electrostatic charge, shape and possibly other currently unknown factors. As a general trend an increased disruption of the fullerene π-system leads to a decrease in the ability of superoxide quenching. In this context monoadducts like **3**, **16**, **51–53** are more effective antioxidants than bisadducts **59** or trisadducts **1**, **14** and **15**. For the different regioisomeric bisadducts **59a–d** the quenching ability is reduced with increasing distance of the addends on the fullerene surface. These observations correlate well with the fact that fullerene derivatives with a more pronounced distortion of the π-system are less efficiently reduced to the corresponding anions. Concerning the electrostatic charge anionic fullerenes like **1–3** and **51–53** seem to be more effective than cationic (**13**, **67** and **68**) or neutral derivatives (**59**, **60**, **62** and **64**). Since there should be stronger electrostatic interaction between the superoxide radical anion and positively charged fullerenes this phenomenon is not fully understood and maybe other factors than redox potential and charge play a major role. For example, the *e*,*e*,*e*-trisadducts **14** and **15** were designed as variants of **1**, but have a very different shape and hydrophobic configuration based on the tethered linker used in their synthesis. Adducts **14** and **15** have similar capacity to **1** as antioxidants against superoxide, but appear to interact with cytochrome C in an entirely different manner from **1**. Electrostatic binding of negatively charged fullerene adducts may cause changes in the absorption characteristics of cytochrome C which could interfere with changes in absorption due to reduction by superoxide determined in the xanthine/xanthine oxidase/cytochrome C assay. This has to be kept in mind upon the careful evaluation of antioxidant properties.

The interactions of fullerenes with cytochrome C may also play an important role in the previously described ability of various fullerenes to protect against apoptotic cell death by physical, chemical and biological toxins.[3–10,14,16–35] Biologically, cytochrome C occupies a critical pathway in cellular redox reactions within both mitochondria and cytosol. Within mitochondria, cytochrome C is a critical component of electron transport and mitochondrial energy production. In the event of a slowdown or disruption of the electron transport chain, the ability of anionic fullerene adducts to bind cytochrome C could conceivably protect the cell from undesired production of oxygen-derived free radicals, including superoxide, hydrogen peroxide, peroxynitrite and hydroxyl radicals. In addition, release of cytochrome C from mitochondria to the cytosol represents a critical and possibly irreversible step in the activation of both apoptotic and non-apoptotic pathways leading to cell death. The ability of fullerenes to bind cytochrome C could conceivably play an important role in

the release of cytochrome C from mitochondria or the ability of cytosolic cytochrome C to trigger cell death pathways. Since water-soluble fullerenes have already been shown to protect against cell death in the presence of a variety of different diseases and toxic insults,[3–5,7–10,16–22,24–28,30,34,35,46–53] our observations with respect to cytochrome C binding raise interesting and important questions with respect to a novel mechanism for cytoprotection by fullerenes.

Conclusions and outlook

In conclusion, our structure–function studies indicate that antioxidant properties of water soluble fullerenes depend on a number of factors, not all of which are completely understood at present. Some of these factors include redox behaviour, charge, size, shape and hydrophobicity. However, within closely related structural families, the similarities of behavior are sufficient to allow a rational approach to design and testing of fullerenes as therapeutic antioxidants. To achieve sufficient water solubility without the aid of a surfactant or co-solvent at least three charges on the addends are required. *In vivo* studies of some of the water soluble fullerene adducts introduced in this study using zebrafish (*Danio rerio*) embryos as model systems reveal that they can protect against chemical toxin-induced apoptotic cell death.[36]

Experimental

Chemicals: C_{60} was obtained from Hoechst AG/Aventis and separated from higher fullerenes by a plug filtration.[54] All chemicals were purchased by chemical suppliers and used without further purification. All analytical reagent-grade solvents were purified by distillation. Dry solvents were prepared using customary literature procedures.[55] Thin layer chromatography (TLC): Riedel-de Haën silica gel F254 and Merck silica gel 60 F254. Detection: UV lamp and iodine chamber. Flash column chromatography (FC): Merck silica gel 60 (230–400 mesh, 0.04–0.063 nm). Analytical high performance liquid chromatography (HPLC): Shimadzu Liquid Chromatograph LC-10 with Bus module CBM-10A, auto injector SIL-10A, two pumps LC-10AT, diode array detector. The HPLC-grade solvents were purchased from SDS or Acros Organics; analytical column Nucleosil 5 µm, 200 × 4 mm, Macherey-Nagel, Düren. Preparative high performance liquid chromatography (HPLC): Shimadzu Class LC 10 with Bus module CBM-10A, auto injector SIL-10A, two pumps LC-8A, UV detector SPD-10A, fraction collector FRC-10A. Solvents were purified by distillation prior to use. UV/Vis spectroscopy: Shimadzu UV-3102 PC UV/Vis/NIR scanning spectrophotometer; absorption maxima λ_{max} are given in nm. Mass spectrometry: Micromass Zabspec, FAB (LSIMS) mode, matrix 3-nitrobenzyl alcohol. NMR spectroscopy: JEOL JNM EX 400 and JEOL JNM GX 400 and Bruker Avance 300. The chemical shifts are given in ppm relative to TMS. The resonance multiplicities are indicated as s (singlet), d (doublet), t (triplet), q (quartet), quin (quintet) and m (multiplet), non-resolved and broad resonances as br. Elemental analysis (C, H, N): succeeded by combustion and gas chromatographic analysis with an EA 1110 CHNS analyser (CE Instruments). **16** was synthesized following the procedure described for **3**.[14] The synthetic procedures and characterization details of the precursor compounds **4**, **20–31**, **37–41**, **54** and **55** and the fullerene compounds **43–47**, **49–53** and **60–64** are available as electronic supplementary information (ESI).†

Superoxide quenching activity assays

Superoxide quenching activity was measured by the method of McCord and Fridovich[44] using xanthine and xanthine oxidase (both obtained from Sigma Aldrich, St. Louis, MO) to generate superoxide radicals and reduction of ferricytochrome C to track the amount and rate of superoxide present in the presence and absence of various fullerenes. Reduced ferricytochrome C was detected by absorbance at 550 nm. Comparable rates of superoxide quenching were observed for several different fullerenes using potassium superoxide and radiolysis-generated superoxide in addition to xanthine/xanthine oxidase generated superoxide.

Photophysics

Fluorescence lifetimes were measured with a Laser Strope Fluorescence Lifetime Spectrometer (Photon Technology International) with 337 nm laser pulses from a nitrogen laser fiber-coupled to a lens-based T-formal sample compartment equipped with a stroboscopic detector. Details of the Laser Strobe systems are described on the manufacture's web site. Emission spectra were recorded with a SLM 8100 Spectrofluorometer. The experiments were performed at room temperature. Each spectrum represents an average of at least 5 individual scans, and appropriate corrections were applied whenever necessary.

1,3,5-Tris((2′-(2″-bromoethyl)malonyl)ethoxy)benzene (7)

DCC (1.39 g, 6.73 mmol) was added to a solution of 1,3,5-tris((2′-hydroxy)ethoxy)benzene **5** (0.50 g, 1.94 mmol), **4** (1.42 g, 31.0 mmol) and 4-DMAP (83 mg, 0.68 mmol) at 0 °C, under N_2 atmosphere and the reaction mixture was stirred for 72 h at room temperature. The solution was filtered and after evaporation of the solvent the residue was dissolved in ethyl acetate and filtered again several times to remove the remaining DCU. Separation by flash column chromatography (SiO_2; toluene/–THF, 4 : 1) gave **7** as a yellow high viscous oil (900 mg, 1.07 mmol, 55%). ^{1}H NMR (400 MHz, rt, $CDCl_3$): $\delta = 6.10$ (s, 3H, Ar*H*), 4.49 (t, $^3J = 4.6$ Hz, 6H, OCH_2CH_2), 4.44 (t, $^3J = 6.1$ Hz, 6H, $BrCH_2CH_2$), 4.15 (t, $^3J = 4.6$ Hz, 6H, OCH_2), 3.49 (t, $^3J = 6.1$ Hz, 6H, $BrCH_2$), 3.48 (s, 6H, $OCCH_2CO$) ppm. ^{13}C NMR (100.5 MHz, rt, $CDCl_3$): $\delta =$ 166.10 (3C, *C*O), 165.81 (3C, *C*O), 160.23 (3C, Ar*C*-O), 94.64 (3C, Ar*C*-H), 65.71 (3C, OCH_2), 64.69 (3C, $BrCH_2CH_2$), 63.68 (3C, OCH_2CH_2), 41.16 (3C, $OCCH_2CO$), 28.03 (3C, $BrCH_2$) ppm. MS (FAB, NBA): $m/z = 836$ $[M]^+$. $C_{27}H_{33}Br_3O_{15}$: calcd C 38.73, H 3.97, Br 28.63, O 28.66; found C 38.20, H 3.99%.

e,*e*,*e*-Trisadduct 10

C_{60} (200 mg, 0.278 mmol) was dissolved in 350 mL of dry and degassed toluene, under an argon atmosphere and vigorous stirring. Subsequently, iodine (275 mg, 1.08 mmol) and **7** (220 mg, 0.263 mmol) were added, followed by the dropwise addition of a solution of DBU (370 µL, 2.48 mmol) in 200 mL of dry toluene over a period of four hours. The reaction mixture was stirred for 20 h at room temperature, filtered through a paper filter to remove the DBU salts and subjected to flash column chromatography on

SiO_2. Elution with toluene afforded traces of unreacted C_{60} and after changing the eluent to toluene–EtOAc 8 : 2 **10** was obtained as a red solid, which was further purified by reprecipitation from $CHCl_3$–pentane and drying under high vacuum (140 mg, 0.090 mmol, 32%). ^{1}H NMR (400 MHz, rt, $CDCl_3$): $\delta = 5.83$ (s, 3H, Ar*H*), 4.84 (d, $^2J = 12.0$ Hz, 3H, OCH_2CH_2), 4.74 (dt, $^2J = 12.0$ Hz, $^3J = 5.8$ Hz, 3H, $BrCH_2CH_2$), 4.59 (dt, $^2J = 12.0$ Hz, $^3J = 5.8$ Hz, 3H, $BrCH_2CH_2$), 4.48 (dd, $^2J = 12.0$ Hz, $^3J = 10.2$ Hz, 3H, OCH_2CH_2), 4.26 (dd, $^2J = 11.5$ Hz, $^3J = 10.2$ Hz, 3H, OCH_2), 4.08 (d, $^2J = 11.5$ Hz, 3H, OCH_2), 3.62 (t, $^3J = 5.8$ Hz, 6 H, $BrCH_2$). ^{13}C NMR (100.5 MHz, rt, $CDCl_3$): $\delta = 162.65$ (3C, *C*O), 162.28 (3C, *C*O), 160.22 (3C, Ar*C*-O), 146.95, 146.89, 146.71, 146.41, 146.36, 146.16, 145.94, 145.71, 145.12, 144.13, 143.56, 143.16, 142.21, 142.03, 141.78, 140.86, 140.82 (54 C, C_{60}-sp^2), 94.05 (3C, Ar*C*-H), 70.47, 69.19 (6 C, C_{60}-sp^3), 66.03 (9C, OCH_2CH_2, $BrCH_2CH_2$), 52.17 (3C, OC*C*CO), 27.95 (3C, Br*C*H$_2$) ppm. MS (FAB, NBA): $m/z = 1552$ [M]$^+$. UV/Vis (CH_2Cl_2): $\lambda_{max} = 251$, 280.5, 304 (sh), 380 (sh), 482, 568 (sh) nm.

e,*e*,*e*-Trisadduct 13

A solution of **10** (50.0 mg, 0.0322 mmol) in 5 mL of dry pyridine was stirred for four days at 60 °C. After the addition of 10 mL of toluene, the reaction mixture was filtrated and the residue was suspended in toluene and distilled under vacuum for several times to remove traces of pyridine. Reprecipitation from methanol–diethyl ether gave **13** (52.3 mg, 0.0292 mmol, 91%). ^{1}H NMR (400 MHz, rt, DMSO-d$_6$): $\delta = 9.19$ (d, $^3J = 6.1$ Hz, 6H, *o*-Pyr*H*), 8.66 (t, $^3J = 7.8$ Hz, 3H, *p*-Pyr*H*), 8.20 (dd, $^3J = 6.1$, 7.8 Hz, 6H, *m*-Pyr*H*), 5.82 (s, 6H, Ar*H*), 5.09 (m, 3H, Pyr-CH_2), 4.98 (m, 3H, Pyr-CH_2CH_2), 4.90 (m, 3H, Pyr-CH_2CH_2), 4.70 (d, $^2J = 12.2$ Hz, 3H, OCH_2CH_2), 4.42 (dd, $^2J = 12.2$ Hz, $^3J = 10.3$ Hz, 3H, OCH_2CH_2), 4.18 (d, $^2J = 11.7$ Hz, 3H, OCH_2), 4.02 (dd, $^2J = 11.7$ Hz, $^3J = 10.3$ Hz, 3H, OCH_2) ppm. ^{13}C NMR (100.5 MHz, rt, DMSO-d$_6$): $\delta = 162.13$ (6C, *C*O), 160.34 (3C, Ar*C*-O), 146.92 (3C, *p*-Pyr*C*), 146.83, 146.78, 146.73, 146.52, 146.23, 146.19, 146.10, 145.75, 145.68 (6C, *o*-Pyr*C*), 145.57, 144.80, 144.03, 143.81, 143.08, 142.51, 141.38, 140.93, 140.92, 140.53 (54 C, C_{60}-sp^2), 128.56 (6C, *m*-Pyr*C*), 94.16 (3C, Ar*C*-H), 70.73, 69.46 (6C C_{60}-sp^3), 66.85 (3C, OCH_2CH_2), 66.15 (6C, O*C*H$_2$, Pyr-CH_2CH_2), 59.32 (3C, Pyr-*C*H$_2$), 52.96 (3C, OC*C*CO) ppm. UV/Vis (CH_2Cl_2): $\lambda_{max} = 265.5$, 285 (sh), 305 (sh), 383 (sh), 480, 568 (sh) nm.

Asymmetric malonate (G1) 36

A solution of **29** (500 mg, 1.65 mmol) and **32** (688 mg, 1.65 mmol) in dry CH_2Cl_2–THF 1 : 1 (150 mL) was cooled to 0 °C under nitrogen atmosphere. DMAP (41 mg, 0.33 mmol), 1-HOBt (223 mg, 1.65 mmol) and EDC (317 mg, 1.65 mmol) were added subsequently. After stirring the solution under N_2 for 2 h at 0 °C, it was left at room temperature for another 24 h. Progress of the reaction was monitored by TLC. The organic phase was washed with water (2 × 100 mL) and dried over $MgSO_4$. After evaporation of the solvent, the resulting product was purified by flash column chromatography (SiO_2, hexane–ethyl acetate, 20 : 15). The purified material was dried under vacuum affording **36** as a colourless oil (716 mg, 1.02 mmol, 62%). ^{1}H NMR (400 MHz, rt, $CDCl_3$): $\delta = 6.01$ (s, br, 1H, CON*H*), 4.16 (t, $^3J = 6.8$ Hz, 2H, OCH_2), 4.14 (t, $^3J = 6.9$ Hz, 2H, OCH_2), 3.32 (s, 2H, $OCCH_2CO$), 2.34 (t, $^3J = 7.5$ Hz, 6H, CH_2COO^tBu), 2.18 (t, $^3J = 7.2$ Hz, 2H, $OCCH_2$), 1.99 (t, $^3J = 7.6$ Hz, 6H, $NHC(CH_2)_3$), 1.62 (m, 6H, CH_2), 1.45 (m, 2H, CH_2), 1.41 (s, 27H, $C(CH_3)_3$), 1.28 (m, 6H, CH_2), 0.89 (t, $^3J = 6.5$ Hz, 3H, CH_3) ppm; ^{13}C NMR (100.5 MHz, rt, $CDCl_3$): $\delta = 172.98$ (3C, *C*OO^{t}Bu), 172.14 (1C, *C*ONH), 166.75 (1C, *C*O), 166.69 (1C, *C*O), 80.44 (3C, *C*(CH$_3$)$_3$), 65.77 (1C, O*C*H$_2$), 65.25 (1C, O*C*H$_2$), 57.34 (1C, NH*C*(CH$_2$)$_3$), 41.58 (1C, OC*C*H$_2$CO), 36.99 (1C, *C*H$_2$CO), 31.33 (1C, *C*H$_2$), 29.87 (3C, NHC(*C*H$_2$)$_3$), 29.63 (3C, *C*H$_2$COO^{t}Bu), 28.36, 28.07 (2C, *C*H$_2$), 28.01 (9C, C(*C*H$_3$)$_3$), 25.98 (1C, *C*H$_2$CH$_2$CO), 25.40, 24.19, 22.55 (3C, *C*H$_2$), 13.95 (1C, *C*H$_3$) ppm. MS (FAB, NBA): $m/z = 700$ [M]$^+$, 528 [M − -3^{t}Bu]$^+$. $C_{37}H_{65}NO_{11}$: calcd C 63.49, H 9.36, N 2.00, O 25.15; found: C 63.12, H 9.44, N 2.03%.

C_{60} monoadduct 42

C_{60} (494 mg, 0.69 mmol) was dissolved in dry toluene (*ca.* 0.5 mL toluene per mg C_{60}) under a nitrogen atmosphere. **36** (400 mg, 0.57 mmol) and CBr_4 (209 mg, 0.63 mmol) were added subsequently. DBU (94 μL, 0.63 mmol) in 50 mL toluene was added dropwise over a period of 1 h to the stirred solution at room temperature. The reaction mixture was stirred at room temperature for an additional 6 h and the progress of the reaction was monitored by TLC. The product was isolated by flash chromatography (SiO_2, toluene–ethyl acetate, 80 : 15 to 80 : 30) and dried under vacuum affording **42** as a red brownish solid (396 mg, 0.28 mmol, 49%). ^{1}H NMR (400 MHz, rt, $CDCl_3$): $\delta = 5.99$ (s, br, 1H, CON*H*), 4.54 (t, $^3J = 6.7$ Hz, 2H, OCH_2), 4.52 (t, $^3J = 6.8$ Hz, 2H, OCH_2), 2.36 (t, $^3J = 7.5$ Hz, 6H, CH_2COO^tBu), 2.22 (t, $^3J = 7.1$ Hz, 2H, $OCCH_2$), 2.00 (t, $^3J = 7.5$ Hz, 6H, $NHC(CH_2)_3$), 1.86 (m, 2H, CH_2), 1.67 (m, 4H, CH_2), 1.49 (m, 2H, CH_2), 1.41 (s, 27H, $C(CH_3)_3$), 1.28 (m, 6H, CH_2), 0.91 (t, $^3J = 6.5$ Hz, 3H, CH_3) ppm; ^{13}C NMR (100.5 MHz, rt, $CDCl_3$): δ = 172.93 (3C, *C*OO^{t}Bu), 172.03 (1C, *C*ONH), 163.66 (1C, *C*O), 163.57 (1C, *C*O), 145.15, 145.14, 145.12, 145.07, 145.05, 145.03, 145.01, 144.76, 144.57, 144.53, 144.52, 144.49, 144.48, 143.75, 142.93, 142.92, 142.88, 142.85, 142.09, 142.05, 141.79, 141.71, 140.86, 140.75, 139.05, 138.89 (58C, C_{60}-sp^2), 80.49 (3C, *C*(CH$_3$)$_3$), 71.78 (2C, C_{60}-sp^3), 67.66 (1C, O*C*H$_2$), 67.28 (1C, O*C*H$_2$), 57.30 (1C, NH*C*(CH$_2$)$_3$), 51.38 (1C, OC*C*CO), 37.09 (1C, *C*H$_2$CO), 31.29 (1C, *C*H$_2$), 29.85 (3C, NHC(*C*H$_2$)$_3$), 29.65 (3C, *C*H$_2$COO^{t}Bu), 28.36, 28.12 (2C, *C*H$_2$), 28.02 (9C, C(*C*H$_3$)$_3$), 25.96 (1C, *C*H$_2$CH$_2$CO), 25.41, 24.20, 22.43 (3C, *C*H$_2$), 13.89 (1C, *C*H$_3$) ppm. MS (FAB, NBA): $m/z = 1442$ [M + Na]$^+$, 1419 [M]$^+$, 720 [C_{60}]$^+$. UV/Vis (CH_2Cl_2): $\lambda_{max} = 254$, 323, 425, 475 nm.

C_{60} monoadduct 48

42 (200 mg, 0.14 mmol) was dissolved in formic acid (20 mL). The reaction mixture was stirred for 24 h at room temperature and the progress of the reaction was monitored by TLC. The reaction mixture was concentrated and purified by reprecipitation from MeOH–Et_2O. Drying under vacuum afforded **48** as a red brownish solid (170 mg, 0.14 mmol, 97%) (broadening of the NMR signals of the deprotected C_{60} monoadducts through aggregation was observed). ^{1}H NMR (400 MHz, rt, DMSO-d$_6$): $\delta = 11.09$ (s, br, 3H, COO*H*), 7.01 (s, br, 1H, CON*H*), 4.49 (m, br, 4H, OCH_2), 2.05 (m, br, 6H, CH_2COOH, $OCCH_2$), 1.79 (m, br, 8H, $NHC(CH_2)_3$, CH_2), 1.51 (m, br, 2H, CH_2), 1.39 (m, br, 8H, CH_2), 1.19 (m, br,

4H, CH_2), 0.88 (m, br, 3H, CH_3) ppm; ^{13}C NMR (100.5 MHz, rt, DMSO-d$_6$): δ = 174.97 (3C, *C*OOH), 171.95 (1C, *C*ONH), 162.87 (1C, *C*O), 162.79 (1C, *C*O), 145.48, 145.01, 144.79, 144.26, 143.56, 143.01, 142.59, 141.71, 141.43, 140.69, 140.42, 139.12, 137.91 (58C, C_{60}-sp^2), 71.59 (2C, C_{60}-sp^3), 67.53 (2C, O*C*H$_2$), 56.99 (1C, NH*C*(CH$_2$)$_3$), 52.03 (1C, OC*C*CO), 37.43 (1C, *C*H$_2$CO), 31.01 (1C, *C*H$_2$), 30.01 (3C, NHC(*C*H$_2$)$_3$), 29.78 (3C, *C*H$_2$COOH), 28.44, 28.22 (2C, *C*H$_2$), 26.01 (1C, *C*H$_2$CH$_2$CO), 25.44, 24.26, 22.39 (3C, *C*H$_2$), 13.98 (1C, *C*H$_3$) ppm. MS (FAB, NBA): m/z = 1250 [M]$^+$, 720 [C_{60}]$^+$. UV/Vis (DMSO): λ_{max} = 252, 322, 424 nm.

C_{60} monoadduct 56

DBU (74.8 µL, 0.50 mmol) was added dropwise to a solution of C_{60} (360 mg, 0.50 mmol), malonate derivative **55** (230 mg, 0.38 mmol) and CBr_4 (134 mg, 0.40 mmol) in dry toluene (250 mL) under a nitrogen atmosphere. The reaction mixture was stirred at room temperature for 20 h and the progress of the reaction was monitored by TLC. The product was isolated by flash chromatography (SiO_2; toluene–ethyl acetate, 90 : 10) and dried under vacuum to afford 200 mg (0.15 mmol, 40%) of a red brownish solid. ^{1}H NMR (400 MHz, rt, $CDCl_3$): δ = 4.62 (t, ^3J = 5.0 Hz, 4H, OCOCH_2), 3.86 (t, ^3J = 5.0 Hz, 4H, OCH_2), 3.74 (t, ^3J = 5.5 Hz, 4H, OCH_2), 3.63 (m, 8H, OCH_2), 3.53 (t, ^3J = 5.5 Hz, 4H, OCH_2), 0.87 (s, 18H, C(CH_3)$_3$, 0.04 (s, 12H, Si(CH_3)$_2$) ppm; ^{13}C NMR (100.5 MHz, rt, $CDCl_3$): δ = 163.48 (2C, *C*O), 145.23, 145.15, 144.87, 144.65, 144.58, 143.85, 143.04, 142.98, 142.95, 142.16, 141.83, 140.89, 139.05 (58C, C_{60}-sp^2), 72.70 (2C, O*C*H$_2$), 71.40 (2C,C_{60}-sp^3), 70.75 (2C, O*C*H$_2$), 70.72 (2C, O*C*H$_2$), 68.76 (2C, O*C*H$_2$), 66.19 (2C, O*C*H$_2$), 62.66 (2C, O*C*H$_2$), 52.03 (1C, OC*C*H$_2$CO), 25.92 (6C, (C(*C*H$_3$)$_3$), 18.35 (2C, (*C*(CH$_3$)$_3$), −5.24 (4C, Si*C*H$_3$) ppm. MS (FAB, NBA): m/z = 1316 [M]$^+$. UV/Vis (CH_2Cl_2): λ_{max} = 254, 322, 423, 475 nm.

C_{60} monoadduct 57

The protected alcohol **56** (100 mg, 0.076 mmol) was dissolved in THF (10 mL) and 2 N HCl (1 mL) was added under vigorous stirring. The progress of the reaction was monitored by TLC. After complete deprotection the solution was diluted with CH_2Cl_2 (50 mL), washed with a saturated solution of $NaHCO_3$ (100 mL) and with water (100 mL). After drying over $MgSO_4$, filtering and concentrating, the product was isolated as a red brownish solid (60 mg, 0.056 mmol, 73%). ^{1}H NMR (400 MHz, rt, $CDCl_3$): δ = 4.63 (t, ^3J = 4.8 Hz, 4H, OCOCH_2), 3.88 (t, ^3J = 4.8 Hz, 4H, OCH_2), 3.72 (m, 8H, OCH_2), 3.65 (4H, OCH_2), 3.58 (m, 4H, OCH_2), 2.96 (s, br, 2H, O*H*) ppm; ^{13}C NMR (100.5 MHz, rt, $CDCl_3$): δ = 163.41 (2C, *C*O), 145.21, 145.12, 145.08, 144.84, 144.62, 144.56, 144.53, 143.82, 143.03, 142.97, 142.92, 142.13, 141.78, 140.87, 139.00 (58C, C_{60}-sp^2), 72.66 (2C, O*C*H$_2$), 71.32 (2C, C_{60}-sp^3), 70.67 (2C, O*C*H$_2$), 70.32 (2C, O*C*H$_2$), 68.65 (2C, O*C*H$_2$), 66.04 (2C, O*C*H$_2$), 61.68 (2C, HO*C*H$_2$), 51.80 (1C, OC*C*CO) ppm. MS (FAB, NBA): m/z = 1109 [M + 2Na]$^+$; 1087 [M + Na]$^+$. UV/Vis (CH_2Cl_2): λ_{max} = 255, 322, 423.5, 475 nm.

C_{60} bisadducts 58a–d

DBU (187 µL, 1.25 mmol) was added dropwise to a solution of C_{60} (360 mg, 0.50 mmol), malonate derivative **55** (627 mg, 1.05 mmol) and CBr_4 (365 mg, 1.10 mmol) in dry toluene (400 mL) under a nitrogen atmosphere. The reaction mixture was stirred at room temperature for 20 h and the progress of the reaction was monitored by TLC. After chromatographic purification (SiO_2; toluene–ethyl acetate, 90 : 10 to 70 : 30; HPLC; toluene–ethyl acetate, 84 : 16) the pure regioisomers were obtained as dark solids. **58a** (*trans*-2) 57 mg (30 µmol, 6%), **58b** (*trans*-3) 124 mg (65 µmol, 13%), **58c** (*trans*-4) 38 mg (20 µmol, 4%), **58d** (*e*) 153 mg (80 µmol, 16%).

58a. ^{1}H NMR (400 MHz, rt, $CDCl_3$): δ = 4.75 (m, 4H, OCOCH_2), 4.60 (m, 4H, OCOCH_2), 3.97 (m, 4H, CH_2OSi), 3.83 (m, 4H, CH_2OSi), 3.74 (m, 12H, OCH_2), 3.68 (m, 4H, OCH_2), 3.61 (m, 8H, OCH_2), .3.57 (m, 4H, OCH_2), 3.53 (m, 4H, OCH_2), 0.87 (s, 18H, C(CH_3)$_3$), 0.86 (s, 18H, C(CH_3)$_3$), 0.05 (s, 12H, Si(CH_3)$_2$), 0.03 (s, 12H, Si(CH_3)$_2$) ppm. ^{13}C NMR (100.5 MHz, rt, $CDCl_3$): δ = 163.87 (2C, *C*O),. 163.44 (2C, *C*O), 147.89, 146.94, 146.28, 146.19, 145.81, 145.59, 145.46, 145.13, 145.08, 144.46, 144.23, 144.16, 144.03, 144.00, 143.67, 143.14, 143.03, 142.97, 142.49, 142.30, 142.21, 142.15, 142.04, 141.60, 140.78, 140.11, 137.71, 137.57 (56C, C_{60}-sp^2), 72.74 (2C, O*C*H$_2$), 72.70 (2C, O*C*H$_2$), 71.43 (4C, C_{60}-sp^3), 70.81, 70.72, 70.70 (8C, O*C*H$_2$), 68.88 (2C, O*C*H$_2$), 68.72 (2C, O*C*H$_2$), 66.33 (2C, O*C*H$_2$), 66.14 (2C, O*C*H$_2$), 62.69 (2C, SiO*C*H$_2$), 62.65 (2C, SiO*C*H$_2$), 49.69 (2C, OC*C*CO), 25.92 (12C, C(*C*H$_3$)$_3$), 18.35 (4C, *C*(CH$_3$)$_3$), −5.24 (8C, Si(*C*H$_3$)$_2$) ppm. MS (FAB, NBA): m/z = 1910 [M]$^+$, 720 [C_{60}]$^+$. UV/Vis (CH_2Cl_2): λ_{max} = 265, 321, 405 (sh), 435, 470 nm.

58b. ^{1}H NMR (400 MHz, rt, $CDCl_3$): δ = 4.63 (m, 4H, OCOCH_2), 4.53 (m, 4H, OCOCH_2), 3.88 (m, 4H, CH_2OSi), 3.77 (m, 4H, CH_2OSi), 3.74 (m, 8H, OCH_2), 3.66 (m, 8H, OCH_2), 3.59 (m, 8H, OCH_2), 3.53 (m, 8H, OCH_2), 0.87 (s, 18H, C(CH_3)$_3$), 0.86 (s, 18H, C(CH_3)$_3$), 0.05, (s, 12H, Si(CH_3)$_2$), 0.03 (s, 12H, Si(CH_3)$_2$) ppm. ^{13}C NMR (100.5 MHz, rt, $CDCl_3$): δ = 163.40 (4C, *C*O), 147.22, 146.95, 146.55, 146.47, 146.41, 146.35, 146.02, 145.96, 145.64, 145.43, 145.29, 144.61, 144.40, 144.15, 143.79, 143.53, 143.36, 142.98, 142.48, 142.29, 142.18, 141.88, 141.59, 140.27, 139.23, 138.58 (56C, C_{60}-sp^2), 72.74 (2C, O*C*H$_2$), 72.70, (2C, O*C*H$_2$), 71.57, 71.08 (4C, C_{60}-sp^3), 70.78, 70.76, 70.73, 70.69 (8C, O*C*H$_2$), 68.79 (2C, O*C*H$_2$), 68.68 (2C, O*C*H$_2$), 66.19 (2C, O*C*H$_2$), 66.10 (2C, O*C*H$_2$), 62.69 (2C, SiO*C*H$_2$), 62.67 (2C, SiO*C*H$_2$), 51.45 (2C, OC*C*CO), 25.94 (12C, C(*C*H$_3$)$_3$), 18.36 (4C, *C*(CH$_3$)$_3$), −5.23 (8C, Si(*C*H$_3$)$_2$) ppm. MS (FAB, NBA): m/z = 1910 [M]$^+$, 720 [C_{60}]$^+$. UV/Vis (CH_2Cl_2): λ_{max} = 251, 310 (sh), 400, 415, 425, 491 (br) nm.

58c. ^{1}H NMR (400 MHz, rt, $CDCl_3$): δ = 4.60 (m, 4H, OCOCH_2), 4.53 (m, 4H, OCOCH_2), 3.85 (m, 4H, CH_2OSi), 3.78 (m, 4H, CH_2OSi), 3.74 (m, 8H, OCH_2), 3.65 (m, 8H, OCH_2), 3.62 (m, 8H, OCH_2), .3.53 (m, 8H, OCH_2), 0.87 (s, 18H, C(CH_3)$_3$), 0.86 (s, 18H, C(CH_3)$_3$), 0.04 (s, 12H, Si(CH_3)$_2$), 0.03 (s, 12H, Si(CH_3)$_2$) ppm. ^{13}C NMR (100.5 MHz, rt, $CDCl_3$): δ = 163.51 (2C, *C*O), 163.44 (2C, *C*O), 148.19, 146.99, 146.49, 146.12, 146.03, 145.56, 145.44, 145.31, 145.09, 145.00, 144.67, 144.17, 143.95, 143.09, 142.94, 142.83, 142.73, 142.22, 142.10, 142.06, 141.86, 141.56, 141.30, 140.92, 140.65, 139.00, 138.48, 135.36 (56C, C_{60}-sp^2), 72.72 (2C, O*C*H$_2$), 72.67, (2C, O*C*H$_2$), 71.02 (4C, C_{60}-sp^3), 70.75, 70.72, 70.70 (8C, O*C*H$_2$), 68.74 (2C, O*C*H$_2$), 68.65 (2C, O*C*H$_2$), 66.09 (2C, O*C*H$_2$), 66.06 (2C, O*C*H$_2$), 62.65 (2C, SiO*C*H$_2$), 62.63 (2C, SiO*C*H$_2$), 49.92 (2C, OC*C*CO), 25.92 (12C, C(*C*H$_3$)$_3$), 18.35 (4C,

$C(CH_3)_3$), −5.24 (8C, Si(CH_3)$_2$) ppm. MS (FAB, NBA): m/z = 1910 [M]$^+$, 720 [C_{60}]$^+$. UV/Vis (CH_2Cl_2): λ_{max} = 244, 316 (sh), 394 (sh), 414, 470.5 (br) nm.

58d. ^{1}H NMR (400 MHz, rt, $CDCl_3$): δ = 4.55 (m, 4H, OCOCH_2), 4.48 (m, 4H, OCOCH_2), 3.79 (m, 8H, CH_2OSi), 3.73 (m, 8H, OCH_2), 3.61 (m, 16H, OCH_2), 3.52 (m, 8H, OCH_2), 0.86, 086 (2s, 18H, C(CH_3)$_3$) 0.03, 0.03 (2 s, 24H, Si(CH_3)$_2$) ppm. ^{13}C NMR (100.5 MHz, rt, $CDCl_3$): δ = 163.43 (1C, *C*O), 163.27 (3C, *C*O), 147.52, 147.23, 146.44, 146.15, 146.04, 145.56, 145.40, 145.13, 145.01, 144.69, 144.58, 144.42, 144.35, 144.02, 143.95, 143.72, 143.69, 143.35, 143.24, 143.15, 142.86, 142.43, 141.82, 141.67, 141.50, 138.77, 138.60 (56C, C_{60}-sp^2), 72.70 (1C, OCH_2), 72.68 (2C, OCH_2), 72.67, (1C, OCH_2), 71.44, 71.34 (3C, C_{60}-sp^3), 70.73, 70.71, 70.70, 70.68 (8C, OCH_2), 70.18 (1C, C_{60}-sp^3), 68.73 (1C, OCH_2), 68.65 (3C, OCH_2), 66.11 (1C, OCH_2), 66.03 (3C, OCH_2), 62.65 (1C, SiOCH_2), 62.63 (3C, SiOCH_2), 53.25 (1C, OC*C*H$_2$CO), 51.11 (1C, OC*C*CO), 25.92 (12C, C(*C*H$_3$)$_3$), 18.36 (4C, *C*(CH$_3$)$_3$), −5.24 (8C, Si(*C*H$_3$)$_2$) ppm. MS (FAB, NBA): m/z = 1910 [M]$^+$, 720 [C_{60}]$^+$. UV/Vis (CH_2Cl_2): λ_{max} = 251, 305 (sh), 401 (sh), 410 (sh), 425, 484 (br) nm.

C_{60} bisadducts 59a–d

The protected alcohol **58a–d** (50 mg, 0.026 mmol) was dissolved in THF (5 mL) and 1 N HCl (1 mL) was added under vigorous stirring. The progress of the reaction was monitored by TLC. After complete deprotection the solution was diluted with CH_2Cl_2 (50 mL), washed with a saturated solution of $NaHCO_3$ (100 mL) and with water (100 mL). After drying over $MgSO_4$ the mixture was concentrated and dried under vacuum for a further 24 h. **59a** (*trans*-2) 26 mg (0.018 mmol, 69%), **59b** (*trans*-3) 27 mg (0.019 mmol, 72%), **59c** (*trans*-4) 24 mg (0.016 mmol, 63%), **59d** (*e*) 28 mg (0.020 mmol, 75%).

59a. ^{1}H NMR (400 MHz, rt, THF-d$_8$): δ = 4.75 (m, 4H, OCOCH_2), 4.58 (m, 4H, OCOCH_2), 3.98 (m, 4H, CH_2OH), 3.84 (m, 4H, CH_2OH), 3.74 (m, 4H, OCH_2), 3.65 (m, 16H, OCH_2), 3.56 (m, 6H, OCH_2), 3.48 (m, 6H, OCH_2), 2.52 (s, br, 4H, OH) ppm. ^{13}C NMR (100.5 MHz, rt, THF-d$_8$): δ = 164.15 (2C, *C*O), 163.76 (2C, *C*O), 149.41, 147.94, 147.17, 146.96, 146.81, 146.32, 146.26, 146.06, 145.86, 145.49, 145.40, 145.08, 145.04, 144.73, 144.52, 144.42, 143.86, 143.31, 143.13, 142.81, 142.46, 141.78, 140.87, 138.69, 138.60 (56C, C_{60}-sp^2), 74.09, 74.03 (4C, OCH_2), 72.80, 72.23 (4C, C_{60}-sp^3), 71.59, 71.55, 71.47 (8C, OCH_2), 69.67, 69.53 (4C, OCH_2), 62.27, 62.23 (8C, HOCH_2), 51.31 (2C, OC*C*CO) ppm. MS (FAB, NBA): m/z = 1453 [M]$^+$, 720 [C_{60}]$^+$. UV/Vis (THF): λ_{max} = 265, 320, 405 (sh), 435, 469 nm.

59b. ^{1}H NMR (400 MHz, rt, THF-d$_8$): δ = 4.63 (m, 4H, OCOCH_2), 4.52 (m, 4H, OCOCH_2), 3.89 (m, 4H, CH_2OSi), 3.79 (m, 4H, CH_2OSi), 3.70 (m, 8H, OCH_2), 3.63 (m, 8H, OCH_2), 3.57 (m, 8H, OCH_2), 3.49 (m, 8H, OCH_2), 2.62 (s, br, 1H, OH) ppm. ^{13}C NMR (100.5 MHz, rt, THF-d$_8$): δ = 163.93 (2C, *C*O), 163.91 (2C, *C*O), 148.40, 148.16, 147.83, 147.73, 147.66, 147.58, 147.51, 147.45, 147.07, 146.69, 146.25, 145.58, 145.38, 145.17, 144.92, 144.66, 144.49, 144.24, 144.15, 143.42, 143.39, 143.38, 142.84, 142.66, 141.31, 140.35, 139.83 (56C, C_{60}-sp^2), 74.15 (2C, OCH_2), 74.11 (2C, OCH_2), 73.10, 72.67 (4C, C_{60}-sp^3), 71.62, 71.60, 71.53 (8C, OCH_2), 69.67 (2C, OCH_2), 69.58 (2C, OCH_2), 62.32 (2C, HOCH_2), 62.30 (2C, HOCH_2), 53.14 (2C, OC*C*CO) ppm; MS (FAB, NBA): m/z = 1453 [M]$^+$, 720 [C_{60}]$^+$. UV/Vis (THF): λ_{max} = 251, 309 (sh), 400, 416, 425, 490 (br) nm.

59c. ^{1}H NMR (400 MHz, rt, THF-d$_8$): δ = 4.57 (m, 4H, OCOCH_2), 4.50 (m, 4H, OCOCH_2), 3.83 (m, 4H, CH_2OH), 3.80 (m, 4H, CH_2OH), 3.64 (m, 8H, OCH_2), 3.59 (m, 8H, OCH_2), 3.53 (m, 8H, OCH_2), .3.46 (m, 8H, OCH_2), 2.52 (s, br, 4H, OH) ppm. ^{13}C NMR (100.5 MHz, rt, THF-d$_8$): δ = 163.77 (2C, *C*O), 163.69 (2C, *C*O), 148.82, 147.82, 147.00, 146.99, 146.63, 146.43, 146.23, 146.08, 146.00, 145.85, 145.77, 145.43, 145.27, 144.80, 144.01, 143.74, 143.71, 143.44, 143.30, 142.95, 142.74, 142.62, 142.17, 141.65, 141.54, 139.93, 139.41, 136.56 (56C, C_{60}-sp^2), 73.93 (2C, OCH_2), 73.89 (2C, OCH_2), 72.27, 71.97 (4C, C_{60}-sp^3), 71.38, 71.35, 71.33 (8C, OCH_2), 69.43 (2C, OCH_2), 69.37 (2C, OCH_2), 62.11 (4C, HOCH_2), 51.43 (2C, OC*C*CO) ppm. MS (FAB, NBA): m/z = 1453 [M]$^+$, 720 [C_{60}]$^+$. UV/Vis (THF): λ_{max} = 245, 316 (sh), 395 (sh), 414, 471 (br) nm.

59d. ^{1}H NMR (400 MHz, rt, THF-d$_8$): δ = 4.53 (m, 8H, OCOCH_2), 4.10 (br, 4H, OH), 3.80 (m, 8H, CH_2OH), 3.63 (m, 8H, OCH_2), 3.56 (m, 16H, OCH_2), 3.48 (m, 8H, OCH_2) ppm. ^{13}C NMR (100.5 MHz, rt, THF-d$_8$): δ = 163.88 (1C, *C*O), 163.83 (1C, *C*O), 163.78 (2C, *C*O), 149.10, 148.10, 147.50, 147.29, 147.27, 147.00, 146.43, 146.27, 146.23, 146.04, 145.87, 145.60, 145.59, 145.52, 145.44, 145.25, 144.92, 144.75, 144.71, 144.70, 144.35, 144.15, 143.77, 143.37, 142.88, 142.60, 142.56, 140.02, 139.45 (56C, C_{60}-sp^2), 74.05 (1C, OCH_2), 74.03 (2C, OCH_2), 74.01 (1C, OCH_2), 72.95, 72.92, 71.67 (4C, C_{60}-sp^3) 71.48, 71.47, 71.46, 71.45 (8C, OCH_2), 69.51 (1C, OCH_2), 69.48 (2C, OCH_2), 69.46 (1C, OCH_2), 62.22 (4C, HOCH_2), 54.95 (1C, OC*C*CO), 52.72 (1C, OC*C*CO) ppm. MS (FAB, NBA): m/z = 1453 [M]$^+$, 720 [C_{60}]$^+$. UV/Vis (THF): λ_{max} = 250, 304 (sh), 401 (sh), 410 (sh), 425, 482 (br) nm.

Oxotetraamino fullerene 67

Trifluoroacetic acid (3.0 mL, 39.0 mmol) was added to a solution of **66** (200 mg, 0.13 mmol) in CH_2Cl_2 (20 mL) under a nitrogen atmosphere. The reaction mixture was stirred for 12 h at room temperature and the progress of the reaction was monitored by TLC. The reaction mixture was concentrated and dried under vacuum to afford 196 mg (124 μmol, 95%) of the product as a orange solid. ^{1}H NMR (400 MHz, rt, MeOD-d$_3$): δ = 8.16 (s, br, 12H, NH), 3.76 (m, 8H, CH_2), 3.00 (m, 12H, CH_2, CH), 2.08 (m, 8H, CH_2), 1.68 (m, 8H, CH_2) ppm. ^{13}C NMR (100.5 MHz, rt, MeOD-d$_3$): δ = 151.60, 151.17, 150.93, 149.53, 149.47, 149.02, 148.73, 148.61, 148.54, 148.37, 147.93, 147.58, 146.86, 146.45, 145.86, 145.79, 145.58, 145.05, 144.97, 144.85, 144.76, 144.70, 142.36, 142.16 (54C, C_{60}-sp^2), 77.80 (1C, C_{60}-sp^3-*C*-O), 76.41 (2C, C_{60}-sp^3-*C*-N), 73.26 (1C, C_{60}-sp^3-*C*-O), 73.19 (2C, C_{60}-sp^3-*C*-N), 51.26 (2C, *C*H$_2$), 50.70 (4C, *C*H$_2$), 50.24 (2C, *C*H$_2$), 47.01 (4C, *C*H), 31.55 (4C, *C*H$_2$), 31.19 (2C, *C*H$_2$), 30.85 (2C, *C*H$_2$) ppm. MS (FAB, NBA): m/z = 1133 [M]$^+$. UV/Vis (MeOH): λ_{max} = 273, 350, 394 nm.

Oxotatraamino fullerene 68

To a solution of **67** (150 mg, 94.0 μmol) in dry MeOH (10 mL) was added $KHCO_3$ (1.0 g, 9.90 mmol) and methyl iodide (6.0 ml,

96.00 mmol) under a nitrogen atmosphere. After the reaction was stirred at room temperature for 72 h the suspension was concentrated and subsequently dissolved in water. After Celite plug-filtration the orange solution was concentrated to a small volume and dialyzed with the aid of dialysis tubes against water for several hours. The molecular weight cut off of the dialysis membranes was 500. After repeated dialysis with replaced water and rotary evaporation, the product was dried under vacuum to afford 51 mg (28.2 μmol, 30%) of the product as an orange solid. ^{1}H NMR (400 MHz, rt, D_2O): δ = 3.76 (m, 12H, CH_2, CH), 3.53 (m, 8H, CH_2), 3.25 (18H, CH_3), 3.19 (18H, CH_3), 2.47 (m, 8H, CH_2), 2.33 (m, 8H, CH_2) ppm. MS (ESI): 795.212 [M + MeOH]$^{2+}$, 488.172 [M + MeOH]$^{3+}$. UV/Vis (H_2O): λ_{max} = 273.5, 346.5, 393 nm.

Acknowledgements

This work was supported by the Deutsche Forschungsgemeinschaft (SFB 583: Redox-aktive Metallkomplexe: Reaktivitätssteuerung durch molekulare Architekturen) and CNI, Houston.

References

1 W. Krätschmer, L. D. Lamb, K. Fostiropoulos and D. Huffman, *Nature*, 1990, **347**, 354–358.
2 A. Hirsch and M. Brettreich, *Fullerenes, Chemistry and Reactions*, Wiley-VCH, Weinheim, 2005.
3 S. S. Huang, S. K. Tsai, L. Y. Chiang, L. H. Chih and M. C. Tsai, *Drug Dev. Res.*, 2001, **53**, 244–253.
4 S. S. Huang, S. K. Tsai, C. L. Chih, L. Y. Chiang, H. M. Hsieh, C. M. Teng and M. C. Tsai, *Free Radical Biol. Med.*, 2001, **30**, 643–649.
5 L. L. Dugan, J. K. Gabrielsen, S. P. Yu, T. S. Lin and D. W. Choi, *Neurobiol. Dis.*, 1996, **3**, 129–35.
6 H. Jin, W. Q. Chen, X. W. Tang, L. Y. Chiang, C. Y. Yang, J. V. Schloss and J. Y. Wu, *J. Neurosci. Res.*, 2000, **62**, 600–607.
7 M. C. Tsai, Y. H. Chen and L. Y. Chiang, *J. Pharm. Pharmacol.*, 1997, **49**, 438–445.
8 H. S. Lai, W. J. Chen and L. Y. Chiang, *World J. Surg.*, 2000, **24**, 450–454.
9 H. S. Lai, Y. Chen, W. J. Chen, J. Chang and L. Y. Chiang, *Transplant Proc.*, 2000, **32**, 1272–1274.
10 Y. L. Lai, H. D. Wu and C. F. Chen, *J. Cardiovasc. Pharmacol.*, 1998, **32**, 714–720.
11 U. Reuther, T. Brandmüller, W. Donaubauer, F. Hampel and A. Hirsch, *Chem.–Eur. J.*, 2002, **8**, 2261–2273.
12 S. Friedman, H. Simon, P. S. Ganapathi, Y. Rubin and G. L. Kenyon, *J. Med. Chem.*, 1998, **41**, 2424–2429.
13 F. Djojo and A. Hirsch, *Chem.–Eur. J.*, 1998, **4**, 344–356.
14 M. Brettreich and A. Hirsch, *Tetrahedron Lett.*, 1998, **39**, 2731–2734.
15 I. Lamparth and A. Hirsch, *J. Chem. Soc., Chem. Commun.*, 1994, 1727–1728.
16 S. Foley, C. Crowley, M. Smaihi, C. Bonfils, B. F. Erlanger, P. Seta and C. Larroque, *Biochem. Biophys. Res. Commun.*, 2002, **294**, 116–119.
17 S. S. Ali, J. I. Hardt, K. L. Quick, J. S. Kim-Han, B. F. Erlanger, T. T. Huang, C. J. Epstein and L. L. Dugan, *Free Radical Biol. Med.*, 2004, **37**, 1191–1202.
18 S. F. Tzeng, J. L. Lee, J. S. Kuo, C. S. Yang, P. Murugan, L. A. Tai and K. C. Hwang, *Brain Res.*, 2002, **940**, 61–68.
19 J. M. Rieger, A. R. Shah and J. M. Gidday, *Exp. Eye Res.*, 2002, **74**, 493–501.
20 A. M. Lin, S. F. Fang, S. Z. Lin, C. K. Chou, T. Y. Luh and L. T. Ho, *Neurosci. Res.*, 2002, **43**, 317–321.
21 L. L. Dugan, E. G. Lovett, K. L. Quick, J. Lotharius, T. T. Lin and K. L. O'Malley, *Parkinsonism Relat. Disord.*, 2001, **7**, 243–246.
22 M. Bisaglia, B. Natalini, R. Pellicciari, E. Straface, W. Malorni, D. Monti, C. Franceschi and G. Schettini, *J. Neurochem.*, 2000, **74**, 1197–1204.
23 J. Lotharius, L. L. Dugan and K. L. O'Malley, *J. Neurosci.*, 1999, **19**, 1284–1293.
24 A. M. Lin, B. Y. Chyi, S. D. Wang, H. H. Yu, P. P. Kanakamma, T. Y. Luh, C. K. Chou and L. T. Ho, *J. Neurochem.*, 1999, **72**, 1634–1640.
25 L. L. Dugan, D. M. Turetsky, C. Du, D. Lobner, M. Wheeler, C. R. Almli, C. K. Shen, T. Y. Luh, D. W. Choi and T. S. Lin, *Proc. Natl. Acad. Sci. U. S. A.*, 1997, **94**, 9434–9439.
26 H. S. Lin, T. S. Lin, R. S. Lai, T. D'Rosario and T. Y. Luh, *Int. J. Radiat. Biol.*, 2001, **77**, 235–239.
27 N. Tsao, T. Y. Luh, C. K. Chou, T. Y. Chang, J. J. Wu, C. C. Liu and H. Y. Lei, *J. Antimicrob. Chemother.*, 2002, **49**, 641–659.
28 N. Tsao, T. Y. Luh, C. K. Chou, J. J. Wu, Y. S. Lin and H. Y. Lei, *Antimicrob. Agents Chemother.*, 2001, **45**, 1788–1793.
29 S. Bosi, T. Da Ros, S. Castellano, E. Banfi and M. Prato, *Bioorg. Med. Chem. Lett.*, 2000, **10**, 1043–1045.
30 T. Mashino, K. Okuda, T. Hirota, M. Hirobe, T. Nagano and M. Mochizuki, *Bioorg. Med. Chem. Lett.*, 1999, **9**, 2959–2962.
31 S. Kiritoshi, T. Nishikawa, K. Sonoda, D. Kukidome, T. Senokuchi, T. Matsuo, T. Matsumura, H. Tokunaga, M. Brownlee and E. Araki, *Diabetes*, 2003, **52**, 2570–2577.
32 D. Monti, L. Moretti, S. Salvioli, E. Straface, W. Malorni, R. Pellicciari, G. Schettini, M. Bisaglia, C. Pincelli, C. Fumelli, M. Bonafe and C. Franceschi, *Biochem. Biophys. Res. Commun.*, 2000, **277**, 711–717.
33 Y. L. Huang, C. K. Shen, T. Y. Luh, H. C. Yang, K. C. Hwang and C. K. Chou, *Eur. J. Biochem.*, 1998, **254**, 38–43.
34 C. Fumelli, A. Marconi, S. Salvioli, E. Straface, W. Malorni, A. M. Offidani, R. Pellicciari, G. Schettini, A. Giannetti, D. Monti, C. Franceschi and C. Pincelli, *J. Invest. Dermatol.*, 2000, **115**, 835–841.
35 E. Straface, B. Natalini, D. Monti, C. Franceschi, G. Schettini, M. Bisaglia, C. Fumelli, C. Pincelli, R. Pellicciari and W. Malorni, *FEBS Lett.*, 1999, **454**, 335–340.
36 F. Beuerle, P. Witte, U. Hartnagel, R. Lebovitz, C. Parng and A. Hirsch, *J. Exp. Nanosci.*, 2007, **2**, 147.
37 F. Beuerle, N. Chronakis and A. Hirsch, *Chem. Commun.*, 2005, 3676–3678.
38 (*a*) M. Braun, A. Atalick, D. M. Guldi, H. Lanig, M. Brettreich, S. Burghardt, M. Hatzimarinaki, E. Ravenelli, M. Prato, R. van Eldik and A. Hirsch, *Chem.–Eur. J.*, 2003, **9**, 3867–3875; (*b*) U. Hartnagel, D. Balbinot, N. Jux and A. Hirsch, *Org. Biomol. Chem.*, 2006, **4**, 1785–1795.
39 M. Brettreich and A. Hirsch, *Synlett*, 1998, **12**, 1396–1398.
40 A. Hirsch, I. Lamparth and H. Karfunkel, *Angew. Chem., Int. Ed. Engl.*, 1994, **33**, 437.
41 A. Herrmann, M. Rüttimann, C. Thilgen and F. Diederich, *Helv. Chim. Acta*, 1995, **78**, 1673.
42 G. Schick, K. D. Kampe and A. Hirsch, *J. Chem. Soc., Chem. Commun.*, 1995, 2023–2024.
43 H. Isobe, T. Tanaka, W. Nakanishi, L. Lemiegre and E. Nakamura, *J. Org. Chem.*, 2005, **70**, 4826–4832.
44 J. M. McCord and I. Fridovich, *J. Biol. Chem.*, 1969, **244**, 6049–6055.
45 D. M. Guldi and K. D. Asmus, *Radiat. Phys. Chem.*, 1999, **56**, 449–456.
46 A. M. Lin, C. H. Yang, Y. F. Ueng, T. Y. Luh, T. Y. Liu, Y. P. Lay and L. T. Ho, *Neurochem. Int.*, 2004, **44**, 99–105.
47 Y. W. Chen, K. C. Hwang, C. C. Yen and Y. L. Lai, *Am. J. Physiol.: Regul. Integr. Comp. Physiol.*, 2004, **287**, R21–26.
48 M. A. Murugan, B. Gangadharan and P. P. Mathur, *Asian J. Androl.*, 2002, **4**, 149–152.
49 D. Y. Yang, M. F. Wang, I. L. Chen, Y. C. Chan, M. S. Lee and F. C. Cheng, *Neurosci. Lett.*, 2001, **311**, 121–124.
50 Y. T. Lee, L. Y. Chiang, W. J. Chen and H. C. Hsu, *Proc. Soc. Exp. Biol. Med.*, 2000, **224**, 69–75.
51 S. C. Chueh, M. K. Lai, M. S. Lee, L. Y. Chiang, T. I. Ho and S. C. Chen, *Transplant Proc.*, 1999, **31**, 1976–1977.
52 B. Puhaca, *Med. Pregl.*, 1999, **52**, 521–526.
53 Y. L. Lai and L. Y. Chiang, *J. Auton. Pharmacol.*, 1997, **17**, 229–235.
54 (*a*) U. Reuther, Ph. D. Dissertation, University of Erlangen-Nürnberg, Germany, 2002; (*b*) L. Isaacs, A. Wehrsig and F. Diederich, *Helv. Chim. Acta*, 1993, **76**, 1231–1250.
55 D. D. Perrin and W. L. F. Amarego, *Purification of Laboratory Chemicals*, 3rd edn, Pergamon Press, Oxford, 1988.